Developing a gillnet based abundance-at-age index for 4RSw Atlantic herring

Mélanie Santo*, Elisabeth Van Beveren*, Kim Émond

*First authors

Maurice Lamontagne Institute, 850 Rte de la Mer, Mont-Joli, QC G5H 3Z4

2025

Canadian Technical Report of
Fisheries and Aquatic Sciences 3733

Fisheries and Oceans Canada Pêches et Océans Canada

Canada

Canadian Technical Report of Fisheries and Aquatic Sciences

Technical reports contain scientific and technical information that contributes to existing knowledge but which is not normally appropriate for primary literature. Technical reports are directed primarily toward a worldwide audience and have an international distribution. No restriction is placed on subject matter and the series reflects the broad interests and policies of Fisheries and Oceans Canada, namely, fisheries and aquatic sciences.

Technical reports may be cited as full publications. The correct citation appears above the abstract of each report. Each report is abstracted in the data base *Aquatic Sciences and Fisheries Abstracts*.

Technical reports are produced regionally but are numbered nationally. Requests for individual reports will be filled by the issuing establishment listed on the front cover and title page.

Numbers 1-456 in this series were issued as Technical Reports of the Fisheries Research Board of Canada. Numbers 457-714 were issued as Department of the Environment, Fisheries and Marine Service, Research and Development Directorate Technical Reports. Numbers 715-924 were issued as Department of Fisheries and Environment, Fisheries and Marine Service Technical Reports. The current series name was changed with report number 925.

Rapport technique canadien des sciences halieutiques et aquatiques

Les rapports techniques contiennent des renseignements scientifiques et techniques qui constituent une contribution aux connaissances actuelles, mais qui ne sont pas normalement appropriés pour la publication dans un journal scientifique. Les rapports techniques sont destinés essentiellement à un public international et ils sont distribués à cet échelon. II n'y a aucune restriction quant au sujet; de fait, la série reflète la vaste gamme des intérêts et des politiques de Pêches et Océans Canada, c'est-à-dire les sciences halieutiques et aquatiques.

Les rapports techniques peuvent être cités comme des publications à part entière. Le titre exact figure au-dessus du résumé de chaque rapport. Les rapports techniques sont résumés dans la base de données *Résumés des sciences aquatiques et halieutiques.*

Les rapports techniques sont produits à l'échelon régional, mais numérotés à l'échelon national. Les demandes de rapports seront satisfaites par l'établissement auteur dont le nom figure sur la couverture et la page du titre.

Les numéros 1 à 456 de cette série ont été publiés à titre de Rapports techniques de l'Office des recherches sur les pêcheries du Canada. Les numéros 457 à 714 sont parus à titre de Rapports techniques de la Direction générale de la recherche et du développement, Service des pêches et de la mer, ministère de l'Environnement. Les numéros 715 à 924 ont été publiés à titre de Rapports techniques du Service des pêches et de la mer, ministère des Pêches et de l'Environnement. Le nom actuel de la série a été établi lors de la parution du numéro 925.

Canadian Technical Report of
Fisheries and Aquatic Sciences 3733

2025

Developing a gillnet based abundance-at-age index for 4RSw Atlantic herring.

by

Mélanie Santo, Elisabeth Van Beveren and Kim Émond

Regional Sciences Branch
Quebec region
Pelagic and Ecosystemic Sciences Division
Fisheries and Oceans Canada
Maurice Lamontagne Institute
850, Route de la Mer
Mont-Joli, QC
G5H 3Z4

Cat. No. Fs97-6/3733E-PDF ISBN 978-0-660-79678-9 ISSN 1488-5379

https://doi.org/10.60825/zcwf-6n63

Correct citation for this publication:

Santo, M., Van Beveren, E. and Émond, K. 2025. Developing a gillnet based abundance-at-age index for 4RSw Atlantic herring. Can. Tech. Rep. Fish. Aquat. Sci. 3733: v + 38 p. https://doi.org/10.60825/zcwf-6n63

TABLE OF CONTENTS

ABSTRACT

Santo, M., Van Beveren, E. and Émond, K. 2025. Developing a gillnet based abundance-at-age index for 4RSw Atlantic herring. Can. Tech. Rep. Fish. Aquat. Sci. 3733: v + 38 p. https://doi.org/10.60825/zcwf-6n63

In 2021, a new experimental gillnet survey was started in Northwest Atlantic Fisheries Organization (NAFO) divisions 4Sw and 4R in collaboration with local harvesters, with the goal of developing a new index of spring and fall spawning Atlantic herring (*Clupea harengus*). This document outlines the survey design, proposes an analytical approach for estimating abundance-at-age indices, and provides an initial assessment of index quality. A new gillnet selectivity model was developed to convert observed length-specific catch rates across multiple mesh sizes into stock abundance-at-length, which was transformed into abundance-at-age using age-length keys. The resulting age compositions successfully tracked dominant cohorts, appeared robust against sample variability in space and time, and aligned with other independent data sources. While the indices appear promising for informing age composition, estimates of overall abundance remain uncertain in part due to limited time series lengths. Additional years of data will help with index validation and clarify its role in future assessments.

RÉSUMÉ

Santo, M., Van Beveren, E. and Émond, K. 2025. Developing a gillnet based abundance-at-age index for 4RSw Atlantic herring. Can. Tech. Rep. Fish. Aquat. Sci. 3733: v + 38 p. https://doi.org/10.60825/zcwf-6n63

En 2021, un nouveau relevé expérimental aux filets maillants a été mis en place dans les divisions 4Sw et 4R de l’ Organisation des pêches de l'Atlantique nord-ouest (OPANO) en collaboration avec des pêcheurs locaux, dans le but de développer un nouvel indice pour les composantes reproductrices de printemps et d’automne du hareng (*Clupea harengus*). Ce document décrit le protocole de relevé, propose une méthode analytique pour estimer les indices d’abondance selon l’âge, et fournit une première évaluation de la qualité de l’indicateur obtenu. Un nouveau modèle de sélectivité des filets maillants a été développé afin de convertir les taux de capture selon la longueur en abondance à la longueur du stock, puis en abondance selon l’âge à l’aide de clés âge-longueur. Les compositions en âge obtenues ont permis de suivre les cohortes dominantes, ont démontré une certaine robustesse face à la variabilité spatiale et temporelle de l’échantillonnage, et sont cohérentes avec d'autres sources de données indépendantes. Bien que les indices semblent prometteurs pour décrire la composition en âge du stock, les estimations d’abondance totale demeurent incertaines, notamment en raison de la courte durée de la série temporelle. La poursuite du relevé permettra de confirmer la robustesse de l’indice et d’en préciser le rôle dans les prochaines évaluations.

1. INTRODUCTION

Atlantic herring (*Clupea harengus*) is a cold-water pelagic species widely distributed throughout the North Atlantic Ocean. In eastern Canadian waters, herring stocks are managed as several distinct units often spanning multiple NAFO (Northwest Atlantic Fisheries Organization) divisions. These management units range from the Scotian Shelf and Bay of Fundy (4VWX), through the southern (4TVn) and northern (4RS) Gulf of St. Lawrence (GSL), and along the coasts of southern and eastern Newfoundland and Labrador (2J3KLPs).

In the northern GSL, as in other western Atlantic stocks, herring comprise two spawning components with localized genetic differentiation (Lamichhaney et al. 2017; Chen et al. 2021): spring spawners (SS) and fall spawners (FS). Stock status of both these northern GSL spawning components has been assessed using data from commercial landings and a summer and fall acoustic survey. However, the interpretation of the key long-term fall acoustic survey has been complicated by delayed herring migration into the sampled area (Chamberland et al. 2022). To reduce assessment uncertainties, a new gillnet survey was introduced in 2021, similar in design to the program established for herring in the southern GSL (Surette et al. 2016). This data expansion also aligns with practices for herring off southern and eastern Newfoundland and Labrador (Wheeler et al. 2010; Bourne et al. 2023), where a scientific gillnet survey likewise contributes valuable information to the regional stock assessment.

In contrast to acoustic surveys, which typically provide a snapshot of stock state at a specific point in time, gillnet surveys can offer broader temporal coverage and may be more resilient to time-varying changes in migration. They generally aim to reflect the abundance and age structure of the recruited population. However, gillnets are inherently size-selective, capturing fish within specific size ranges depending on mesh dimensions. To mitigate this bias (e.g., Shoup and Ryswyk 2016), gillnet surveys typically employ multi-panel nets with different mesh sizes, allowing for a more representative sampling of the population. A multi-panel design also enables the estimation of mesh-specific size selectivity and, in turn, reconstruction of the underlying length distribution of the stock (Millar and Holst 1997; Millar and Freyer 1999). For instance, Surette et al. (2016) successfully used a gillnet selectivity model to derive a length-specific, and by extension, age-specific abundance index for southern GSL herring. Although the northern GSL gillnet program has now accumulated four years of data, these must still be synthesized into formal indicators to support stock assessment efforts.

Science advice and management of northern GSL herring have traditionally been structured by NAFO division (4R and 4S; DFO 2021, 2022a). However, recent acoustic tagging work (Émond and Nilo 2025) has confirmed that herring from 4Sw routinely migrate into 4R during fall, and return to 4Sw shelf waters in spring. Consistent age structures observed across both divisions in commercial landings and acoustic surveys (DFO 2023, 2024) further support the view that these represent a single biological unit. Accordingly, new gillnet indices should reflect this biological reality.

This technical report aims to develop a new abundance-at-age index for northern GSL SS and FS herring and evaluate possible uncertainties. We provide recommendations for future survey efforts and the integration of this index into the stock assessment process. The goal is to work towards model-based integration of multiple indicators of stock state.

2. METHODS

2.1 SAMPLE DESIGN

In 2021, an experimental gillnet survey was initiated in collaboration with local fishermen from various NAFO unit areas (4Ra, 4Rc, and 4Sw) (Figure 1). Sampling covered the spring and fall spawning season: from around mid-May to the end of June (spring) and from early August to the end of September each year (fall, including post-spawning in 4R) (Figure 2).

From 2021 to 2024, a total of eight harvesters were contracted annually and instructed to collect at least one sample per week over a period of four consecutive weeks for each sampling period (spring and fall). The same harvesters participated each year and were only replaced when necessary by others from the same area. Each harvester was provided a standardized multi-panel gillnet, consisting of five equidimensional panels (7.3 m long and 5.2 m deep) joined sequentially in ascending order of mesh size; 2, $2^{1/4}$, $2^{1/2}$, $2^{3/4}$ and 3 inches (in 2021, a $2^{5/8}$-inch mesh was used instead of the 3-inch panel). The nets were made of monofilament nylon and featured a 10 mm diameter 3-strand polypropylene lead-core rope equipped with 25 evenly spaced 2 x 5 inch rubber oval floats. Harvesters were asked to target potential spawning sites where herring abundance was expected to be high (Figure 1). Gillnets were set at depths ranging from 5.5 to 36.6 m and soak times generally ranged from 10 to 30 hours, although the protocol indicates a 24 h maximum (Figure 3). For each haul, harvesters completed a logbook to record metadata (e.g., date, position, set and haul time) as well as the total weight of herring caught per panel, which was either estimated by the harvester or measured using a scale. A random sample of up to 50 fish (30 fish in 2021) from each panel was boxed and shipped to the Maurice Lamontagne Institute (MLI). For nearly all events (99%), the sample size equalled the total catch per panel.

At MLI, a technician estimated for each fish its total length (± 1 mm), total weight (± 1 g), gonad weight (± 0.1 g), sex, gonad development stage, and age from otolith extraction and examination. Individuals were assigned to a spawning component (SS or FS) based on their gonad maturity stage and sample date (see Émond et al. 2024). Frozen fish weight and gonad weight were converted to fresh weight using the standard equations for this stock assessment (Émond et al. 2024). A very small number of fish arrived at MLI in very poor condition and were discarded. One sample collected outside the target period (July) was removed from the database, and all samples collected in 4Rd (St. George's Bay) had to be excluded due to data quality issues, including lack of panel separation and transport-related sample degradation. The total number of samples and fish collected by year, season, and NAFO unit area are presented in Table 1, while annual fish counts by mesh size and spawning component are shown in Table 2.

2.2 DATA ANALYSES

2.2.1 Abundance-at-length

The observed number of herring ($n_{i,c,m,l}$) per sampling event (i), spawning component (c; SS or FS), mesh size (m), and length class (l) was first standardized to the panel surface area (S_m in m^2), soak time (T_i in hours), and the sampling ratio (total fish weight $W_{i,m}$ over sampled weight $w_{i,m}$), according to the following equation:

$$N_{i,c,m,l} = \frac{n_{i,c,m,l} * W_{i,m}}{S_m * T_i * w_{i,m}} \quad (1)$$

When the total catch weight equaled the sample weight, the catch weight was corrected to reflect the laboratory-measured sample weight. The resulting standardized abundance, $N_{i,c,m,l}$, was averaged across sample events, to obtain abundances ($\bar{N}_{y,r,c,m,l}$) by year (y; 2021-2024), region (r; 4R and 4Sw), spawning component, mesh size, and length class. Two regions were defined in the analysis to allow region-specific age-length keys, assess potential regional effects (related to biological or sampling differences), and facilitate comparison with previous datasets. Note that larger catches contributed proportionally more to the stratum-specific length distributions. The baseline standardized counts ($\bar{N}_{y,r,c,m,l}$) were then input into a gillnet selectivity model to integrate length frequencies across the different mesh sizes (Figure 4 and 5). The effect of mesh-selectivity is demonstrated in Figure 6, where $\bar{N}_{y,r,c,m,l}$ was averaged by length class, mesh size and spawning component.

2.2.2 Gillnet selectivity model

A new gillnet selectivity model was developed using the Template Model Builder (TMB; Kristensen et al. 2016) package in R (R Core Team 2025), building on the statistical framework established by Millar and Holst (1997) and extended by Surette et al. (2016). Millar and Holst (1997) developed the basis for the most widely used gillnet selectivity model (e.g., as implemented in the TropFishR package; Mildenberger et al. 2025), which estimates mesh-specific selectivity and infers the underlying length distribution of a stock. Surette et al. (2016) expanded this framework to enable estimation of abundance-at-length across multiple strata at once, assuming constant mesh-specific selectivity curves. A stratum can be defined as any unique combination of for instance sampling year, period, region, and spawning component. Surette et al. (2016) focused on abundance estimation by year and region. Here, we further develop their method. The use of TMB streamlined the estimation process and enabled straightforward computation of confidence intervals for any quantity derived from the model. The full code, validated using the TropFishR demo dataset, is publicly available at iml-assess/gillnetTMB.

The model was based on the following equation:

$$\log(\bar{N}_{s,m,l}) = \log(\lambda_{s,l}) + \log(Sel_m(L_l)) + \varepsilon_{s,m,l} \quad (2)$$

where $\lambda_{s,l}$ is the relative abundance of the stock for stratum s by length class l, and $Sel_m(L_l)$ is the mesh-specific selectivity function for each length class, independent of time and space. Note that in contrast to Surette et al. (2016), all nets were by default assumed to have equal fishing power, with no mesh-specific scaler applied. Available data from both our survey and the southern GSL were inadequate to support reliable estimation of such a scaling parameter.

We integrated two types of count distributions, continuous variants of the Poisson and negative binomial (see Surette et al. 2016), and four log-linear selectivity curves (see Millar and Holst 1997): normal with fixed spread, normal with spread scaled to mesh size, gamma, and lognormal (Appendix 1). Models were optimized using the nlminb function from the R “stats” package. For every data input scenario, including base runs and sensitivity tests, all eight possible combinations of count distributions and selectivity curves were tested and the model with the lowest Akaike Information Criterion (AIC) was selected. Convergence diagnostics for the selected model included checks for successful optimization, a low maximum gradient component (<0.001), and a positive definite Hessian matrix. Model fit was further evaluated through residual plots.

Models were run separately for SS and FS, as selectivity-at-length may differ between these stock components due to variations in their availability to the nets (driven by migratory behaviour and environmental conditions) as well as morphological differences such as body condition. Sampling year (2021-2024) and region (4Sw and 4R) were defined as strata. Due to limited data, seasonal stratification was not added, and no strong biological justification was identified for selecting only spawning season samples for each spawning component (e.g., restricting the index for SS to spring data). For instance, there is no consistent pattern in spawning component composition between seasons (e.g., spring samples are not consistently dominated by SS). Although gillnet selectivity models are traditionally based on count data, low catch rates and extended soak times (see Eq. 1 and Figure 3) resulted in input values that were generally too small (<1) to support standard count distributions. To address this, input values ($\overline{N}_{s,m,l}$) were multiplied by a factor of 1,000 and rounded to the nearest whole number prior to model fitting; abundance predictions ($\lambda_{s,l}$) were then converted back to their original scale. To facilitate model convergence, we also ensured length classes with zero observations within a given stratum (defined by year, region, and mesh size) were excluded. Additionally, the dataset was zero-padded within a stratum for length classes that were only observed in a subset of mesh sizes.

2.2.3 Abundance-at-age

The model-estimated abundance-at-length per stratum ($\lambda_{s,l}$) was subsequently transformed into abundance-at-age ($\lambda_{s,a}$) based on year and region-specific age-length keys. Note that it would have also been possible to directly use observed abundances-at-age as model input and apply an age rather than length-based selectivity model. A length-based selectivity framework was however preferred, as mesh selection acts on fish shape rather than age, and this method aligns with standard practices, enabling comparison with the southern GSL.

Based on the biological data from the experimental gillnet survey, annual age-length keys were constructed by region (4R and 4Sw) for SS and FS, following

$$p(l|a)_s = \frac{\sum_i n_{s,i,l,a}}{\sum_i \sum_a n_{s,i,l,a}} \quad (3)$$

where the numerator represents the number of aged herring by length class across all sampling events in a given strata, and the denominator is the total fish number per stratum and length class. The multinom function from the nnet R package (Venables and Ripley 2022) was applied to impute missing values and produce smoothed age-length keys. As age readings for 4R in 2024 were still pending at the time of writing, 4Sw data were applied to this stratum.

Herring abundances-at-length were then multiplied by these keys. Summing the number of fish across lengths, by age and stratum (including years and regions), provided abundance-at-age indices:

$$\lambda_{s,a} = \sum_{l=1}^{L} \left(\lambda_{s,l} * p(l|a)_s\right) \quad (4)$$

Regional estimates can be summed to produce annual relative abundance-at-age indices for 4RSw herring. However, this aggregation could be biased if survey catchability differs among regions or over time (e.g., if harvesters in one region fish more efficiently).

2.3 EVALUATION OF UNCERTAINTIES

Stock indicators are inherently associated with multiple potential sources of uncertainty. This section explores some of these and provides context for interpreting the indicator. The results are also intended to support future planning and improvements to the survey program and statistical analyses.

We acknowledge that the current time series is relatively short and that some analyses should be revisited as additional years of data become available.

2.3.1 Fish body condition

Gillnets are selective for fish shape, and length is only a proxy for the underlying traits that govern fish retention (e.g., Carol and García-Berthou 2007). Consequently, if fish shape changes over time independently of length, gillnet selectivity may also vary, violating a key assumption of the selectivity model. One potential solution to this would be to measure fish girth directly (e.g., Kurkilahti et al. 2002). However, such data are unavailable for northern GSL herring and most other stocks, primarily due to the measurement's labour-intensive nature and low precision. To indirectly evaluate whether selectivity-at-length might vary over time, we examined trends in fish body condition. Significant temporal trends in this parameter might introduce bias into the abundance estimates.

Relative body condition of SS and FS herring in the commercial and acoustic survey databases was estimated using Le Cren's (1951) body condition index:

$$K_a^{rel} = \frac{W_a}{k * {L_a}^b} \tag{5}$$

where W_a is the annual age-specific somatic fish weight (g), L_a the corresponding total fish length (mm), and k and b are the parameters of the average logarithmic weight-length relationship. A K_a^{rel} value below one indicates that fish, for their length class, are underweight relative to the historical mean. The condition indices were standardized to account for seasonal, spatial and gear variability between samples using GLMs (see Émond et al. 2024 for details).

2.3.2 Spatial survey coverage

The gillnet survey covers a broad geographic area, with samples collected across multiple NAFO unit areas. However, the sampling effort in each unit area varies both within and between years, and the number of sampling events together with the number of fish caught in each event are insufficient to fully account for these fluctuations. For example, the number of sampling events and the sample sizes from 4Ra compared to 4Rc has varied from 2021 to 2024 (Table 1), but in some strata, data are insufficient (e.g. no samples or few fish) to reliably apply standard area-specific weighting procedures. This variability in spatial coverage may introduce bias in the presented indicators if population abundance or structure differs meaningfully at finer spatial scales, which might be expected (e.g., Eliasen et al. 2021).

For future sample collection, it is also valuable to evaluate the optimal spatial resolution. Specifically, it remains unclear whether comprehensive coverage of all NAFO unit areas is necessary—this is associated with considerable administrative and transportation costs—or whether increased sampling frequency in a few key areas (e.g., 4Ra) would better represent the entire stock, recognizing that herring are expected to migrate through certain NAFO unit areas en route to more southern areas (Émond and Nilo 2025).

To better understand stock structure at a finer spatial scale, we compared the annual age composition of SS and FS herring between NAFO unit areas 4Ra and 4Rc. This analysis was based on available biological samples collected during the gillnet survey window (June to September) from both the commercial fleet and the summer acoustic survey. Annual proportions-at-age were calculated by averaging across random samples within each unit area. Note that to have sufficient sample numbers, the result reflects the age composition of herring caught in a variety of mobile gear types (pelagic trawl, bottom trawl and seiners), without accounting for differences in their selectivity.

2.3.3 Temporal survey coverage

A similar source of uncertainty relates to the imbalance in temporal coverage of the survey. Sampling was conducted during two distinct periods of the year: spring and late summer to early fall. To evaluate whether seasonal differences in sampling influenced the results, we used the survey data itself, and reran the selectivity model with strata redefined to include season while excluding 4R because of limited data (Table 1). This approach assumes that length-selectivity remains constant between periods. The estimated seasonal abundances-at-age were then visually compared.

2.3.4 Catch-curve analysis

An effective age-structured abundance index should show cohort abundances decline across successive years as a function of total mortality, provided gear selectivity effects are appropriately accounted for. Catch curves were therefore plotted as the logarithmic abundances of each cohort over time, for 3 to 12 year old herring. The slope of the lines gives an estimate of total mortality rate, and is anticipated to be downwards.

Abundance-at-age indices contain information on two components of a stock's dynamics: (1) the structure (i.e., proportions-at-age) and (2) the total abundance (i.e., $\lambda_{y,a} = p_{y,a}\lambda_y$). The catch-curve analysis can help evaluate whether the observed signal in the index provides reliable information on both components, or whether only the former should be considered, or possibly the abundance at a subset of ages (e.g., a recruitment index, as in Bourne et al. 2023).

2.3.5 Consistency with other surveys

We compared trends in the new gillnet index with established indicators. Consistency across independent data sources strengthens confidence in the new index and supports its inclusion into an integrated assessment model. Specifically, proportions-at-age from the gillnet survey were compared with those from the summer and fall acoustic surveys, as well as with commercial catch-at-age data (see Émond et al. 2024). Total abundance estimates were only compared with the summer acoustic survey.

3. RESULTS AND DISCUSSION

3.1 ABUNDANCE-AT-LENGTH

The standardized abundances-at-length used as model input (Figures 4 and 5), and averaged across strata for visualization (Figure 6), demonstrated a clear pattern of size-selectivity across mesh sizes. Overall, input values were extremely low, regardless of location, timing, or spawning component. On average, standardized abundances in 4RSw were roughly two orders of magnitude lower compared to herring in the southern GSL (see Figure 5 in Surette et al. 2016), where spawning aggregations are likewise targeted, and after accounting for the absence of standardization for panel size in that area. One key difference is soak time: while nets in the 4T survey where typically deployed for about an hour (and up to 10 hours), harvesters in 4RSw routinely soaked nets for 10 to 30 hours, with a 24-hour set being most common (Figure 3). This difference reflects the fishing strategies employed; while the 4T fishery focused on actively targeting dense spawning aggregations, local harvesters in 4RSw relied on traditional knowledge of the stock to determine net placement in a predetermined area.

3.2 GILLNET SELECTIVITY MODEL

The best-fitting models used a Poisson distribution and applied a scaled normal selectivity curve for SS, and a gamma selectivity curve for FS (Table 3). Residual plots (Figure 7) indicated as expected an overall linear relationship between predicted and observed values. However, while general trends were captured, the predicted versus observed plot showed considerable variability around the 1:1 line, including notable overestimation where observed values were near zero. These patterns resulted from the low number of herring caught per stratum; small samples inevitably produced noisy input distributions (Figures 4 and 5). Sampling limitations were most apparent at the distribution tails, where low fish counts introduced greater uncertainty.

Selectivity curves estimated independently for SS and FS were broadly similar (Figure 8). Across mesh sizes, peak selectivity occurred at fish lengths that differed by 0.5 to 1 cm (Table 4). Most panels selected FS at sizes only slightly smaller than SS (by 1 cm or less). The selectivity curves for FS were considerably wider, indicating that the nets retained a wider range of fish lengths for this component. This might be driven by the slightly wider range of lengths observed for FS (Figures 4-6).

Compared to results from the southern GSL (Figure 9), where the gillnet survey is conducted in August and September, selectivity curves for FS in the northern GSL were shifted toward larger fish sizes and exhibited greater variance. Differences in selectivity were evident already in the raw length-frequency data (Figure 6; Figure 5 in Surette et al. 2016), suggesting this significant difference is not merely the result of sample size or model selection. Importantly, fish larger than 35 cm were also commonly captured in the northern GSL, but were absent from the southern GSL catches. This comparison underscores the importance of developing region- and stock-specific selectivity curves when constructing abundance indices based on gillnet survey data.

Model-estimated abundances-at-length, stratified by year and region, were associated with wide confidence intervals, particularly in NAFO Division 4R, where overall abundance was lowest for both spawning components (Figures 10 and 11). Uncertainty was most pronounced at the extremes of the length distributions.

3.3 ABUNDANCE-AT-AGE

Total relative abundance of both SS and FS declined over the four years of the survey (Figure 12). This decline was largely driven by reductions in 4Sw, where the majority of herring were caught in most years.

Despite regional differences in total abundance trend, the annual age composition of herring was strikingly similar between 4R and 4Sw for both spawning components (Figure 13). Although total abundance in 4R was lower (Figure 12) and estimated length-at-age in this region was associated with wider confidence intervals (Figures 10 and 11), this did not translate into noticeably more diffuse cohort patterns in the 4R bubble plots (Figure 13). In both regions, the same cohorts were dominant and herring were caught ranging from ages 3 to 11 for SS and up to age 12 for FS. Tracking cohorts through time was generally more straightforward for SS than for FS, even though sampling effectiveness appeared comparable for both components (Figures 12 and 13).

For SS, the 2017 cohort (age 4 in 2021) was particularly dominant, whereas for FS, the 2016 cohort (age 5 in 2021) stood out as the most prominent, with no other cohorts showing similarly strong signals across survey years. For both components, older age classes (age 10 and above) were relatively well represented in the gillnet survey.

3.4 EVALUATION OF UNCERTAINTIES

3.4.1 Fish body condition

From 1970 to 2024, the body condition of both SS and FS herring has fluctuated on an interannual basis, but with no clear evidence of a long-term trend (Figures 14 and 15). This pattern holds across all age classes. However, during the final four years of the time series, corresponding to the period covered by the gillnet survey, considerable year-to-year variability in fish condition remained evident, particularly among SS herring. Body condition of older age classes was significantly lower in or around 2024 compared to 2022. Indeed, condition estimates during this period were accompanied by non-overlapping confidence intervals.

Shifts in body condition of SS individuals in 2023 and 2024 could introduce some bias in the indicator. Because the gillnet selectivity curve estimated by the model and used to convert observed to stock abundance represents an average across the survey period, it does not account for potential trends in vulnerability to the gear that may be associated with directional changes in fish condition. Quantifying this potential bias is currently challenging, primarily due to the limited duration of the survey time series.

We recommend that fish condition time series be maintained and updated alongside the gillnet survey index. If a trend in condition emerges over time and a longer survey time series becomes available, future analyses could for instance consider estimating separate selectivity curves for blocks of years with similar fish condition. Such an approach would enable the evaluation of time-varying selectivity and its contribution to overall uncertainty in the index. At present, annually estimated selectivity curves would be too imprecise to identify whether changes reflect true biological shifts or artifacts arising from insufficient data.

Further exploration of the relationship between fish condition and mesh selectivity could be achieved by integrating data across regions, such as including results from the southern GSL.

3.4.2 Spatial survey coverage

Commercial and acoustic survey samples collected during the gillnet survey period demonstrated that both SS and FS herring exhibited highly similar age structures across unit areas 4Ra and 4Rc (Figure 16). There was for instance no clear indication that older fish travelled further, as is common in small pelagic fish species (e.g., Nøttestad et al. 1999). An imbalance in finer-scale spatial coverage, such as between subregions 4Ra and 4Rc, is therefore unlikely to introduce significant bias into age compositions observed in the gillnet survey. Key conclusions, including cohort tracking and indications of age truncation, would remain largely unaffected by small-scale spatial sampling variation.

Across all years and both spawning components, absolute differences in age composition between 4Ra and 4Rc generally remained below 10% (79% of all comparisons). Some variance might be attributed to the mixture of gear types. The largest discrepancies were further associated with years where the number of fish analysed was relatively low (e.g., SS in 2024).

3.4.3 Temporal survey coverage

Consistent temporal coverage appeared more critical for FS than for SS in producing robust age composition estimates (Figure 17). For SS herring, age structures observed in spring samples were highly similar to those obtained in summer, with temporal differences falling within the range of expected observation error. This suggests that, for SS, changes in sampling season had minimal influence on our perception of cohort strength.

In contrast, FS herring cohorts were difficult to distinguish in the spring proportions-at-age. Although the number of FS captured during this period was generally low, the inability to detect typically present dominant cohorts persisted even in years of relatively high sample numbers (e.g., 2022), and when cohort structure was more clearly visible in summer. Older cohorts tended to be more dominant in spring, except in 2024, when younger cohorts were more prevalent. Summer sampling might provide a more reliable depiction of the age composition of the entire FS component, as it aligns more closely with other stock indicators (see results below). Note that Figure 17 was generated under the assumption that gillnet selectivity does not vary by season. While this may be a simplification of reality, it is not expected to have a major influence on cohort tracking.

3.4.4 Catch-curve analysis

Catch-curve analyses for 4Sw, and more broadly for the combined 4RSw region, generally showed downward-sloping patterns for both SS and FS, consistent with expectations of declining abundance due to cumulative mortality with age (Figure 18). This pattern was relatively stable across the 2021–2023 period but became less consistent between 2023 and 2024. Between those last two years, especially the youngest cohorts increased in relative abundance, which may reflect residual issues in the estimation of abundance for younger age classes. Due to typically low sample sizes at these ages, despite small mesh panels, the gillnet selectivity model has limited ability to correct for these observation errors. Nonetheless, catch-curve analyses for the combined 4RSw region generally supported a consistent downward trend, suggesting that the gillnet survey index retains potential value as an indicator of relative abundance for stock assessment purposes.

In region 4R, where overall herring abundance was lower, catch curves were generally close to horizontal, suggesting implausibly low or even slightly positive mortality rates. This pattern indicates inconsistencies in cohort structure and considerable observation error, potentially due to very weak catch rates and hence high variability in catchability. Consequently, the relative abundance of SS and FS herring in 4R, as estimated from the gillnet survey alone, is unlikely to provide a reliable representation of true stock abundance in its current state.

3.4.5 Consistency with other surveys

The age composition of SS and FS herring estimated from the gillnet survey accounts for gear selectivity from age 3 onwards. In contrast, age compositions derived from the commercial fishery (catch-at-age) and the summer acoustic survey still reflect the selectivity of the respective gears, in addition to the stock's age structure. For these indicators, gear selectivity is often estimated when integrating them into a stock assessment model. For the presented comparison, we did not apply any selectivity correction to the commercial or acoustic data, as such assumptions are uncertain and likely to change in future assessment cycles.

Despite methodological differences, there was consistency among all three indicators in tracking the dominant 2017 cohort for SS herring and the 2016 cohort for FS herring (Figure 19). Because gear selectivity is explicitly accounted for in the gillnet index, the estimated abundances were however more evenly distributed across all age classes. Notably, the gillnet index consistently produced higher estimates of older herring relative to the other two indicators. This pattern may reflect a positive bias in the gillnet survey toward older individuals or, alternatively, some degree of dome-shaped selectivity in the acoustic and commercial data. The latter might however be less likely, given that purse seines (the primary gear used in the commercial fishery) and pelagic trawls (used in the acoustic survey) are generally not known to underrepresent larger fish. Moreover, there are no known spatial refuges where larger herring would be consistently unavailable to these gears. In contrast, the proportional importance of older herring could be overestimated when gillnet selectivity curves have some degree of bias. In terms of younger fish (ages 1 and 2), these were more frequently captured in the commercial fishery and the acoustic survey, making them potentially more informative for detecting early signs of recruitment. Overall, integrating age composition information from all three indicators (gillnet, commercial, and acoustic) should yield a more robust and precise estimation of age composition.

Total abundance of both SS and FS herring in 4RSw, as estimated from the gillnet survey, showed a general decline over the four-year period (Figure 20). While this downward trend does not directly contradict the pattern observed in the summer acoustic survey, the two indices do not exhibit parallel trajectories. Although no major inconsistencies were identified that would preclude the use of the gillnet survey as an index of relative abundance, the short duration of the time series limits a full evaluation of its ability to reliably track overall stock trends. Continued data collection will be essential to assess its performance over time and to determine its appropriate role within a stock assessment model (e.g., necessity for downweighing).

4. CONCLUSION

The results presented in this document support the intended use of the gillnet survey as a new indicator of SS and FS herring stock state in 4RSw. While the time series is short and uncertainties remain, the data showed internal spatio-temporal consistency in terms of reflected age structure, as well as reasonable alignment with other independent indicators. No issues emerged from basic quality control checks (e.g., catch-curve analyses). These results suggest that the index is on track to contribute meaningfully to upcoming stock assessments, particularly for informing age structure and cohort tracking.

Determining how to best incorporate the gillnet survey indices into the stock assessment is an ongoing process, likely to evolve as the time series expands and new insights emerge. Approaches vary across regions. In Newfoundland, herring gillnet data are used either as an index of recruitment or as a full age-disaggregated abundance index (Bourne et al. 2023), whereas in the southern GSL, an equivalent index has been used solely to inform proportions-at-age (DFO 2022b). Given that in the current study only four years of data were available, the quality of age compositions were more easily assessed than total abundance. The survey effectively captured major cohorts, albeit with more consistent results for SS than FS herring. While the age structure information appears robust, trends in total abundance remain more uncertain, as they tend to be more sensitive to sample variability (e.g., Wheeler et al. 2010), and quality control is mostly limited to catch curves (or similar mortality based approaches) and comparisons with independent indicators. Continued data collection and testing different integration approaches into a full assessment model will be key to evaluating its utility.

Low catch rates, especially in 4R, reduced the precision of both age compositions and abundance estimates. Addressing this issue is challenging: increasing survey effort could improve precision but would require additional resources, while shifting effort towards higher yield areas or periods could compromise survey consistency, which is critical for detecting trends over time. Doing so could also make the survey more sensitive to potential shifts in herring migration. Note that the number of targeted samples in the 4RSw survey is already comparable to the gillnet survey in the southern GSL (Surette et al. 2016). Although Newfoundland region generally contracts more than twice the number of harvesters to conduct their gillnet survey (Wheeler et al. 2010), the workload appears balanced by for instance sending fewer fish for analysis. The observed low catch rates in 4RSw may reflect genuinely low herring abundance during the surveyed period or they might result from the survey design. The relationship between soak time and catch rate is particularly relevant in this context. Although a linear relationship is assumed, catch rates may not increase proportionally with soak duration due to factors such as gear saturation, fish avoidance over time, escapement, and predation (e.g., Prchalová et al. 2011; Li et al. 2011). At present, gear saturation (low catch rates) and predation (unreported by harvesters) are considered unlikely to affect catch rates. Additional sources of survey variability, such as set depth or cohort maturation, may also impact results, but their influence is not yet fully understood. Better understanding these factors might help refine index standardization and improve the interpretation of low catch rates.

REFERENCES

Bourne, C., Squires, B., O'Keefe, B., and Schofield, M. 2023. Assessment of Newfoundland East and South Coast Atlantic Herring (*Clupea harengus*) Stock Complexes to 201. Can. Sci. Advis. Secr. Res. Doc. **2023/013**: iv + 41p.

Carol, J., and García-Berthou, E. 2007. Gillnet selectivity and its relationship with body shape for eight freshwater fish species. J. Appl. Ichthyol. **23**(6): 654–660. doi:10.1111/j.1439-0426.2007.00871.x.

Chamberland, J.-M., Lehoux, C., Vanier, C., Smith, S., Lacroix-Lepage, C., Paquet, F., Benoît, H.P., Van Beveren, E., and Plourde, S. 2022. Atlantic herring (*Clupea harengus*) stocks of the west coast of Newfoundland (NAFO Division 4R) in 2019. Can. Sci. Advis. Secr. Res. Doc. **2021/076**: v + 115 p.

Chen, J., Bi, H., Pettersson, M.E., Sato, D.X., Fuentes-Pardo, A.P., Mo, C., Younis, S., Wallerman, O., Jern, P., Molés, G., Gómez, A., Kleinau, G., Scheerer, P., and Andersson, L. 2021. Functional differences between TSHR alleles associate with variation in spawning season in Atlantic herring. Commun. Biol. **4**(1): 795. doi:10.1038/s42003-021-02307-7.

Le Cren, E.D. 1951. The Length-Weight Relationship and Seasonal Cycle in Gonad Weight and Condition in the Perch (*Perca fluviatilis*). J. Anim. Ecol. **20**(2): 201–219. doi:10.2307/1540.

DFO. 2021. Assessment of the Quebec North shore (division 4s) herring stocks in 2020. Can. Sci. Advis. Secr. Sci. Advis. Rep. **2021/037**: 15.

DFO. 2022a. Assessment of the west coast of Newfoundland (NAFO Division 4R) herring (*Clupea harengus*) stocks in 2021. Can. Sci. Advis. Secr. Sci. Advis. Rep. (2022/020): 18.

DFO. 2022b. Assessment of the southern Gulf of St. Lawrence (NAFO division 4TVn) spring and fall spawner components of Atlantic herring (*Clupea harengus*) with advice for the 2022 and 2023 fisheries. Can. Sci. Advis. Secr. Sci. Advis. Rep. **2022/021**: 38.

DFO. 2023. Update of stock status indicators for Quebec North Shore (Division 4S) herring in 2022. Can. Sci. Advis. Secr. Sci. Response **2023/032**.

DFO. 2024. Stock Status Update of West Coast of Newfoundland (NAFO Division 4R) Herring for the 2024 and 2025 Fishing Seasons. Can. Sci. Advis. Secr. Sci. Response **2024/020**.

Eliasen, S.K., Homrum, E.Í., Jacobsen, J.A., Kristiansen, I., Óskarsson, G.J., Salthaug, A., and Stenevik, E.K. 2021. Spatial Distribution of Different Age Groups of Herring in Norwegian Sea, May 1996–2020. Front. Mar. Sci. **8**. doi:10.3389/fmars.2021.778725.

Émond, K., Dionne, H., Beaudry-Sylvestre, M., Paquet, F., Rousseau, S., Lehoux, C., and Nilo, P. 2024. Assessment of the West Coast of Newfoundland (NAFO Division 4R) Atlantic Herring (*Clupea harengus*) Stocks in 2021. Can. Sci. Advis. Secr. Res. Doc. **2024/004**: xi + 93p.

Émond, K., and Nilo, P. 2025. Preliminary Results from an Acoustic Telemetry Study on Atlantic Herring in the Northern Gulf of St. Lawrence. Can. Sci. Advis. Secr. Res. Doc. (2025/029): iv + 24p.

Kristensen, K., Nielsen, A., Berg, C.W., Skaug, H., and Bell, B.M. 2016. TMB: Automatic Differentiation and Laplace Approximation. J. Stat. Softw. **70**(5): 1–21. doi:10.18637/jss.v070.i05.

Kurkilahti, M., Appelberg, M., Hesthagen, T., and Rask, M. 2002. Effect of fish shape on gillnet selectivity: a study with Fulton's condition factor. Fish. Res. **54**(2): 153–170. doi:10.1016/S0165-7836(00)00301-5.

Lamichhaney, S., Fuentes-Pardo, A.P., Rafati, N., Ryman, N., McCracken, G.R., Bourne, C., Singh, R., Ruzzante, D.E., and Andersson, L. 2017. Parallel adaptive evolution of geographically distant herring populations on both sides of the North Atlantic Ocean. Proc. Natl. Acad. Sci. **114**(17). doi:10.1073/pnas.1617728114.

Li, Y., Jiao, Y., and Reid, K. 2011. Gill-Net Saturation in Lake Erie: Effects of Soak Time and Fish Accumulation on Catch per Unit Effort of Walleye and Yellow Perch. North Am. J.

Fish. Manag. **31**(2): 280–290. doi:10.1080/02755947.2011.574931.
Mildenberger, T.K., Taylor, M.H., and Wolff, M. 2025. TropFishR: Tropical Fisheries Analysis (version 1.6.6). Available from https://github.com/tokami/TropFishR.
Millar, R.B., and Freyer, R.J. 1999. Estimating the size-selection curves of towed gears, traps, nets and hooks. Rev. Fish Biol. Fish. **9**: 89–116. doi:https://doi.org/10.1023/A:1008838220001.
Millar, R.B., and Holst, R. 1997. Estimation of gillnet and hook selectivity using log-linear models. ICES J. Mar. Sci. **54**(3): 471–477. doi:10.1006/jmsc.1996.0196.
Nøttestad, L., Giske, J., Holst, J.C., and Huse, G. 1999. A length-based hypothesis for feeding migrations in pelagic fish. Can. J. Fish. Aquat. Sci. **56**(S1): 26–34. doi:10.1139/f99-222.
Prchalová, M., Mrkvička, T., Peterka, J., Čech, M., Berec, L., and Kubečka, J. 2011. A model of gillnet catch in relation to the catchable biomass, saturation, soak time and sampling period. Fish. Res. **107**(1–3): 201–209. doi:10.1016/j.fishres.2010.10.021.
R Core Team. 2025. R: A language and environment for statistical computing. R Foundation for Statistical Computing. Vienna, Austria. Available from http://www.r-project.org/.
Shoup, D.E., and Ryswyk, R.G. 2016. Length Selectivity and Size-Bias Correction for the North American Standard Gill Net. North Am. J. Fish. Manag. **36**(3): 485–496. doi:10.1080/02755947.2016.1141809.
Surette, T., LeBlanc, C., and Mallet, A. 2016. Abundance indices and selectivity curves from experimental multi-panel gillnets for the southern Gulf of St. Lawrence fall herring fishery. Can. Sci. Advis. Secr. Res. Doc. **067**: vi + 23 p.
Venables, W.N., and Ripley, B.D. 2022. Modern Applied Statistics with S. Springer, New York.
Wheeler, J.P., Squires, B., and Williams, P. 2010. An assessment framework and review of Newfoundland east and south coast herring stocks to the spring of 2009. Can. Sci. Advis. Secr. Res. Doc. **2010/020**: 132.

5. TABLES

Table 1 : Number of sampling events (N) and number of fish (n) collected per year, sampling period (spring or fall), and NAFO unit area. No stock differentiation was made (spring versus fall herring). Sampling periods were defined as spring (May-June) and fall (August-September). A dash (“-”) indicated no samples were collected.

	4Ra		4Rc		4Sw	
	N	n	N	n	N	n
2021	-	-	4	56	21	513
spring	-	-	4	56	9	358
fall	-	-	-	-	12	155
2022	6	542	4	122	16	1612
spring	-	-	4	122	8	1143
fall	6	542	-	-	8	469
2023	6	598	4	109	16	916
spring	-	-	4	109	6	141
fall	6	598	-	-	10	775
2024	2	184	3	19	17	1078
spring	-	-	3	19	8	299
fall	2	184	-	-	9	779

Table 2 : Number of fish collected per spawning component, mesh size (inch), NAFO unit area, and year. Grey cells indicate data is unavailable.

	Spring spawners						Fall spawners					
	2	$2^{1/4}$	$2^{1/2}$	$2^{5/8}$	$2^{3/4}$	3	2	$2^{1/4}$	$2^{1/2}$	$2^{5/8}$	$2^{3/4}$	3
4Ra												
2021												
2022	114	43	25		11	0	92	77	79		73	28
2023	86	57	41		24	3	102	110	107		58	10
2024	23	21	26		5	0	28	33	23		23	2
4Rc												
2021	3	0	0	10	4		0	0	0	27	12	
2022	0	12	26		24	3	0	6	8		23	20
2023	0	8	17		5	4	0	4	5		14	52
2024	0	6	4		6	0	1	2	0		0	0
4Sw												
2021	57	61	48	38	18		30	28	75	85	73	
2022	365	197	168		54	28	113	171	178		23	20
2023	155	83	29		6	3	106	107	158		176	93
2024	195	169	98		32	4	85	126	139		134	93

Table 3 : Gillnet selectivity model output for each spawning component. The model with the lowest Akaike information criterion (AIC) is indicated in bold. (df = degrees of freedom, MGC = maximum gradient component, conv = convergence).

Spring spawners								
	Poisson				Negative Binomial			
	Normal scaled	Normal fixed	Lognorm	Gamma	Normal scaled	Normal fixed	Lognorm	Gamma
AIC	**-2894.92**	-2844.20	NA	-2873.39	-2467.22	-2448.71	NA	-2457.04
df	**193**	193	NA	193	194	194	NA	194
MGC	**<0.001**	<0.001	NA	<0.001	<0.001	<0.001	NA	0.28
k1	**5.524**	5.418	NA	92.624	5.506	5.382	NA	117.258
k2	**0.309**	3.402	NA	0.060	0.243	3.025	NA	0.046
Conv	**ok**	ok	x	ok	ok	ok	x	ok
Fall spawners								
	Poisson				Negative Binomial			
	Normal scaled	Normal fixed	Lognorm	**Gamma**	Normal scaled	Normal fixed	Lognorm	Gamma
AIC	-4182.10	-4172.84	NA	**-4197.51**	-3297.40	-3308.30	NA	-3298.05
df	226	226	NA	**226**	227	227	NA	227
MGC	<0.001	<0.001	NA	**<0.001**	<0.001	<0.001	NA	0.37
k1	5.453	5.349	NA	**67.590**	5.470	5.340	NA	103.673
k2	0.417	4.022	NA	**0.081**	0.274	3.295	NA	0.053
Conv	ok	ok	x	**ok**	ok	ok	x	ok

Table 4 : Estimated fish length (cm) at maximum gillnet selectivity, by mesh size (inch) and spawning component.

Mesh size (inch)	Fish length (cm)	
	Spring spawners	Fall spawners
2	28	27.5
2 1/4	31.5	31
2 1/2	35	34.5
2 5/8	37	36
2 3/4	38.5	37.5
3	42	41

6. FIGURES

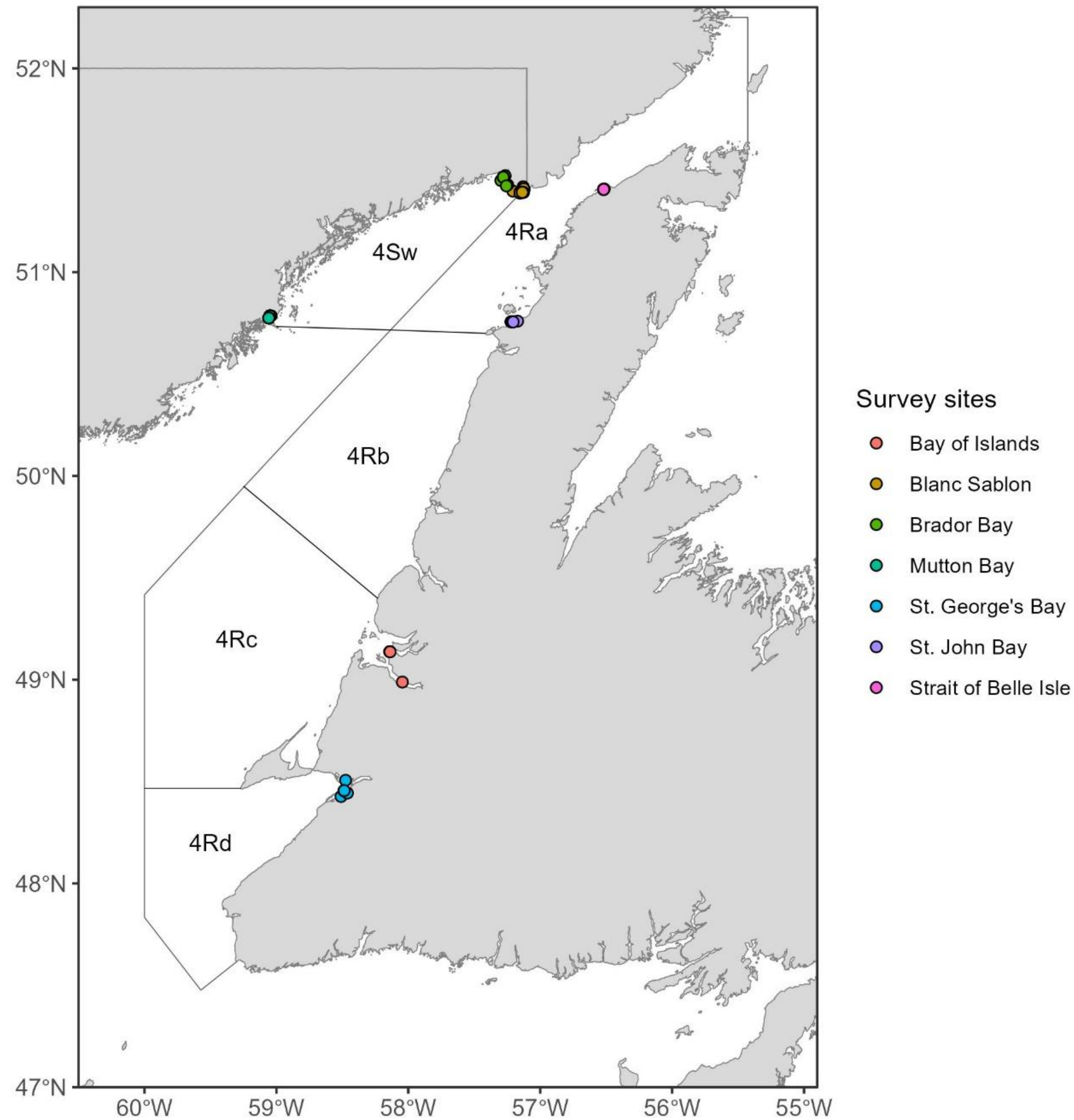

Figure 1 : Survey sites of the herring gillnet survey with indication of NAFO unit areas. Samples from St. George's Bay (4Rd) were excluded from the analysis owing to incomplete data.

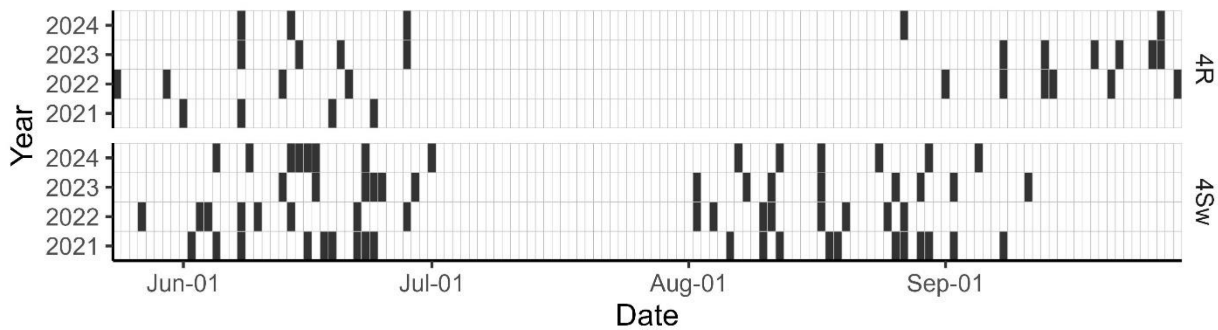

Figure 2 : Haul date of gillnet samples per region and year.

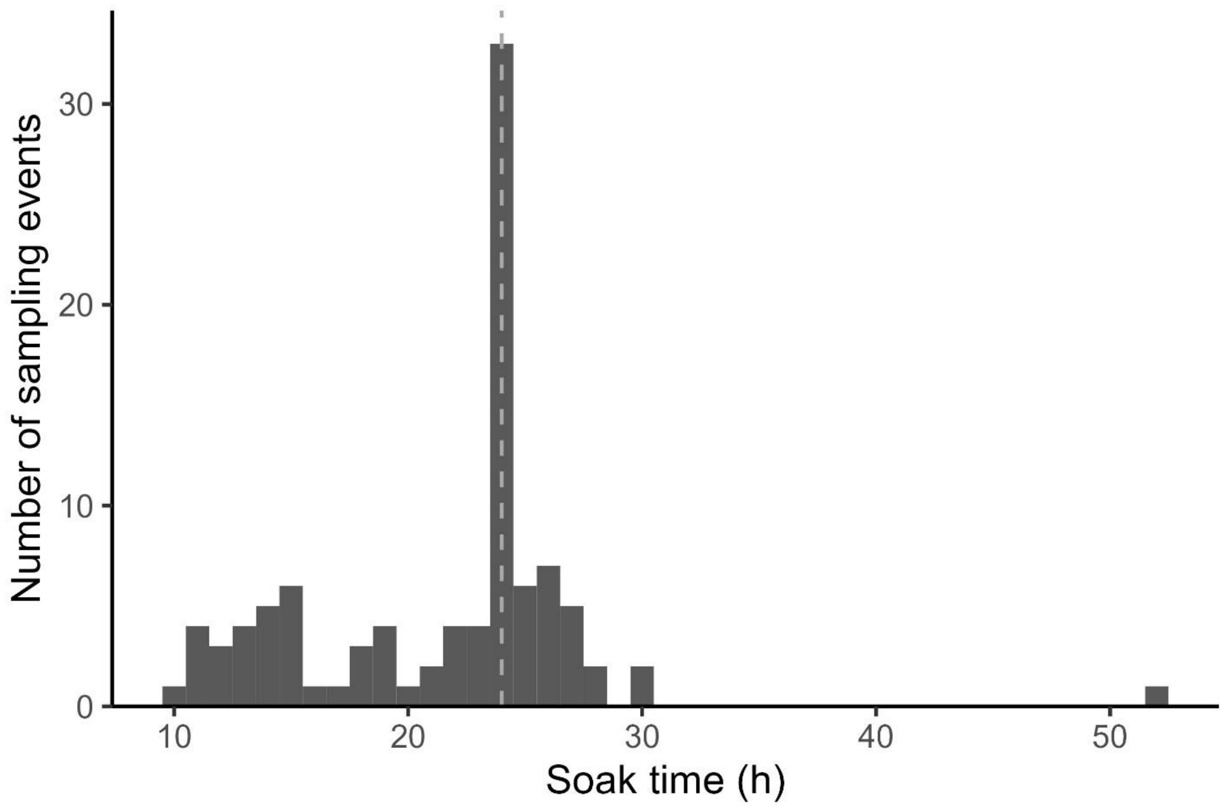

Figure 3 : Histogram of soak times across all years and areas. Soak times exceeding the 24-hour protocol limit (dashed vertical line) were retained in the analysis.

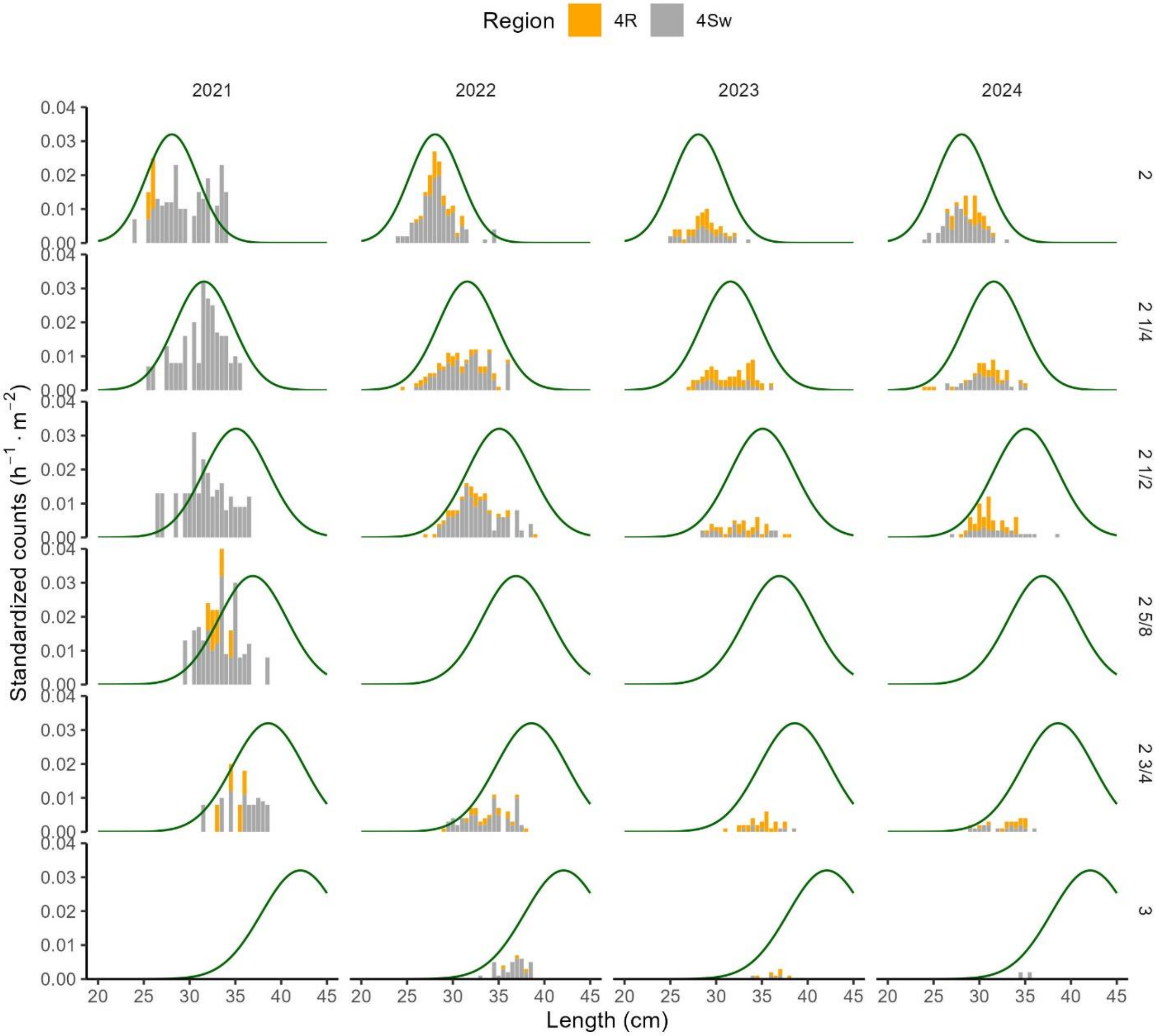

Figure 4: Standardized counts of spring spawning herring ($h^{-1} \cdot m^{-2}$) caught per length class (cm), mesh size (inch; rows), year (columns) and region (colours). Data are used as input into the gillnet selectivity model. Green curves are estimated selectivity curves (normal scaled; see Table 3) scaled to the maximum observed counts.

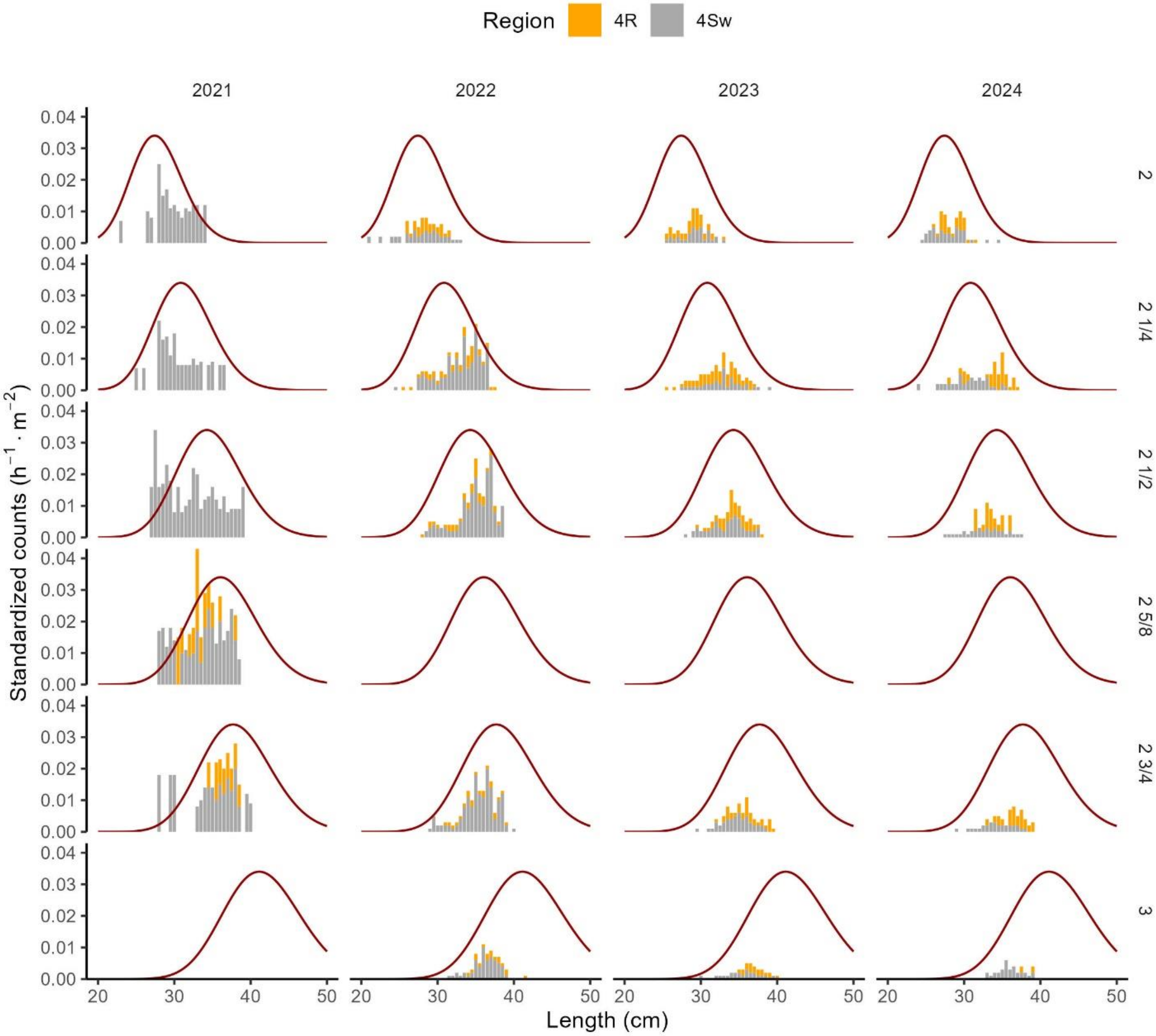

Figure 5: Standardized counts of fall spawning herring ($h^{-1} \cdot m^{-2}$) caught per length class (cm), mesh size (inch; rows), year (columns) and region (colours). Data are used as input into the gillnet selectivity model. Red curves are estimated selectivity curves (gamma; see Table 3) scaled to the maximum observed counts.

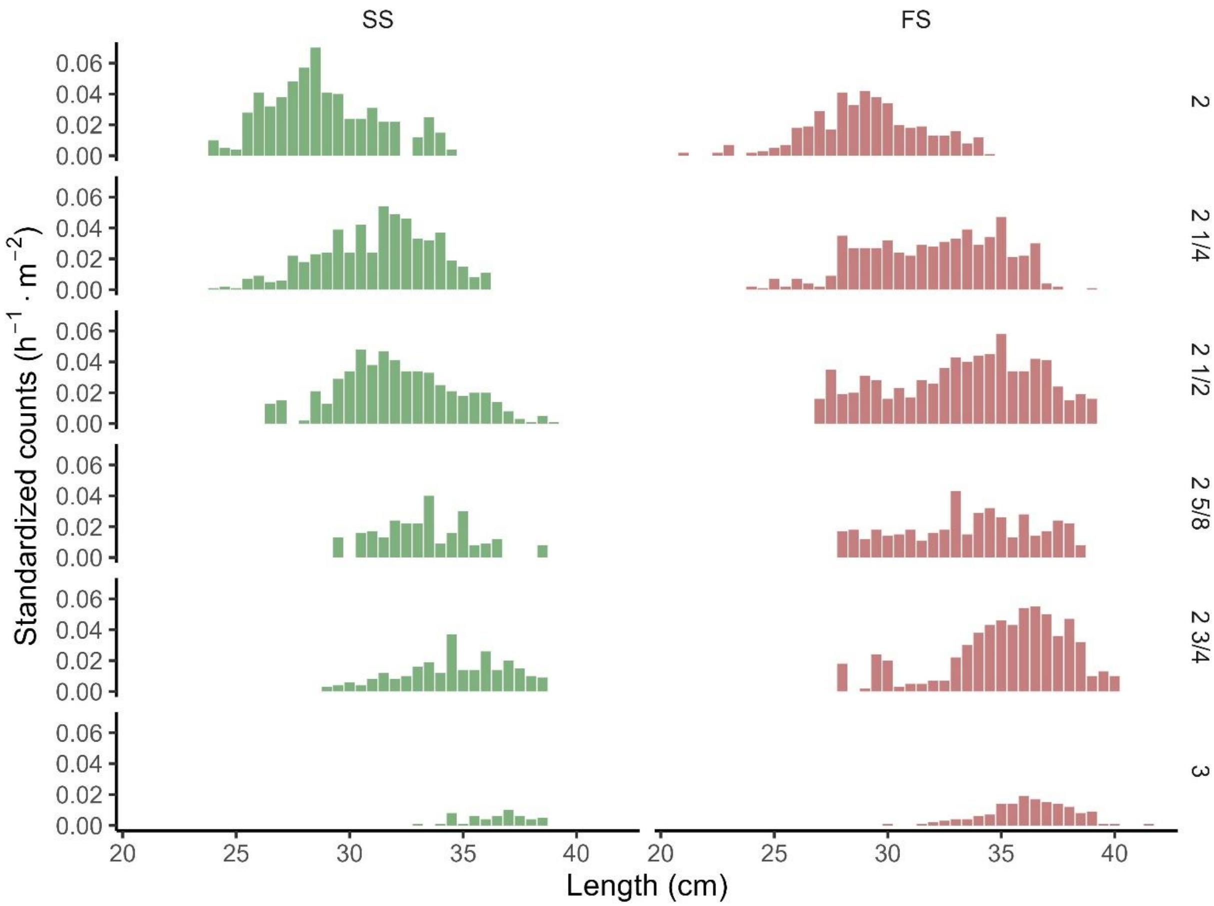

Figure 6 : Standardized counts of herring ($h^{-1} \cdot m^{-2}$) caught per length class (cm), mesh size (inch; rows), and spawning component (columns; SS = spring spawners; FS = fall spawners). Values were averaged across all years and regions.

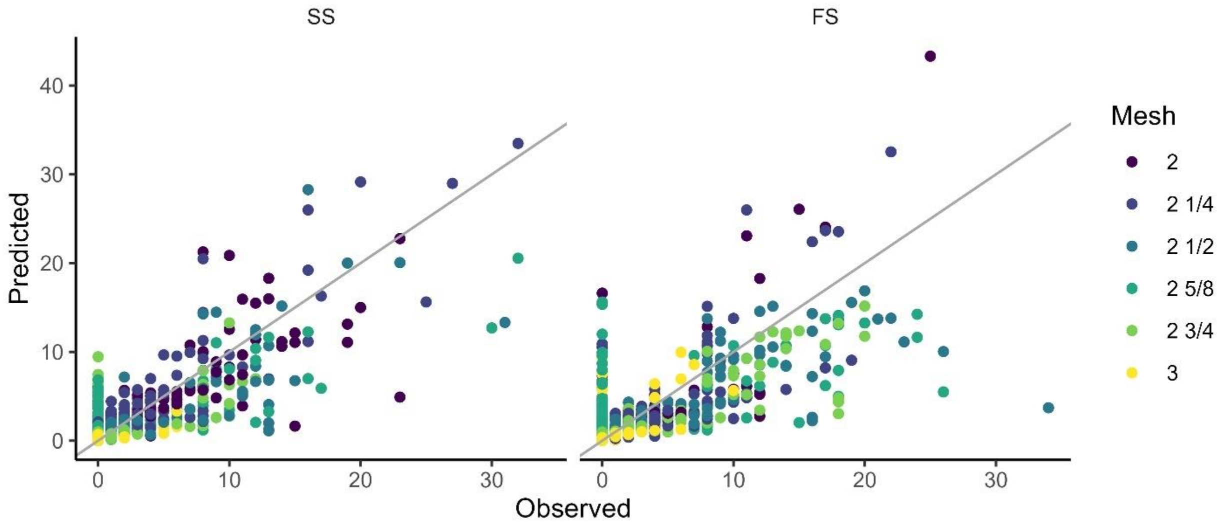

Figure 7 : Observed versus predicted standardized herring counts ($h^{-1} \cdot m^{-2} \cdot 1000$) from the gillnet selectivity model, applied to spring (SS) and fall spawners (FS).The grey line shows the 1:1 ratio.

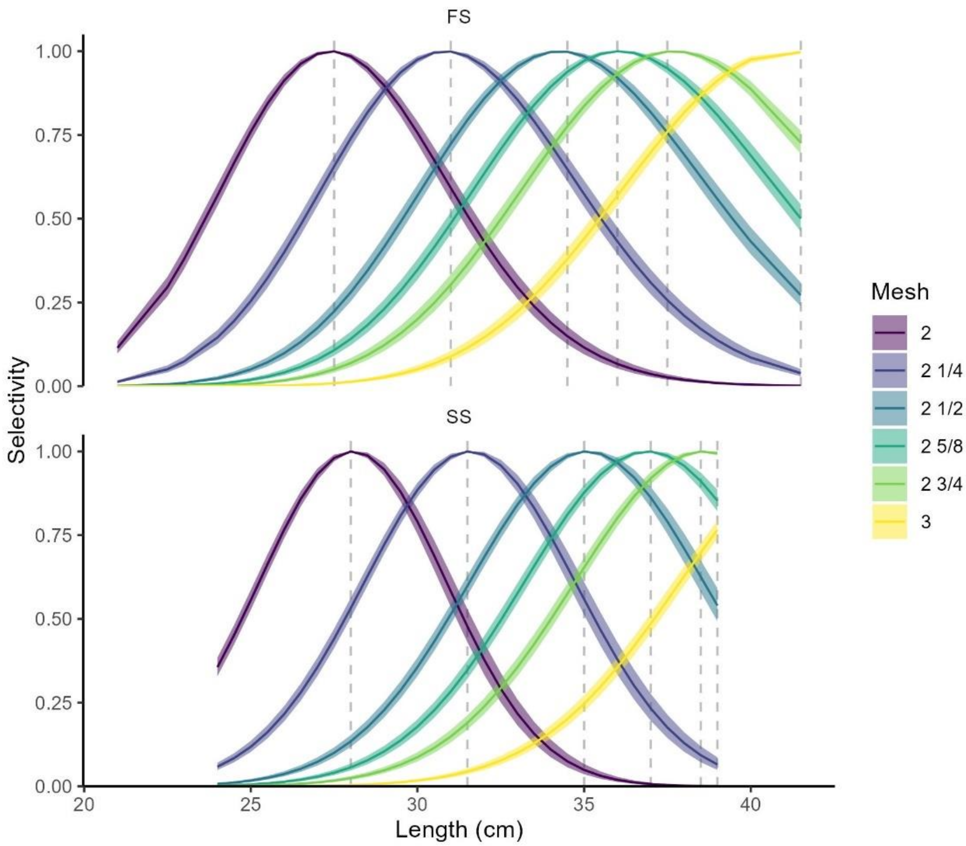

Figure 8 : Predicted gillnet selectivity per mesh size (inch) for fall (FS) and spring spawners (SS). For spring spawners curves follow a scaled normal distribution and for fall spawners curves follow a gamma distribution. The vertical dashed lines indicate length at peak gillnet selectivity (Table 4).

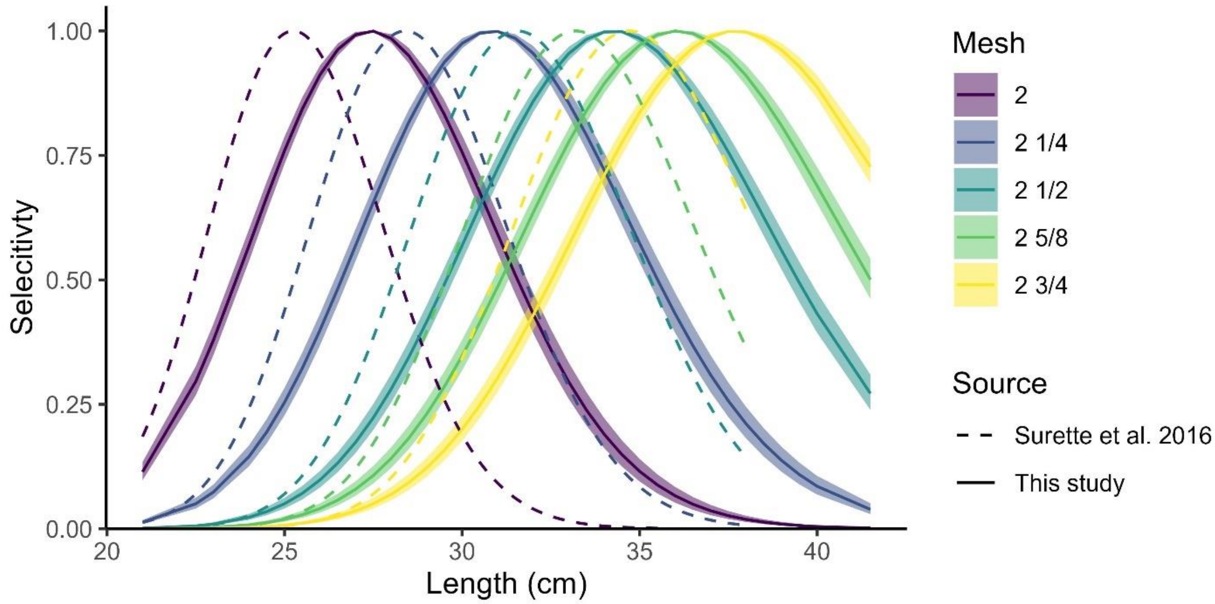

Figure 9 : Gillnet selectivity curves for fall spawners estimated in this study (4RSw herring) and by Surette et al. (2016; 4T herring). Only mesh sizes used in both surveys were included.

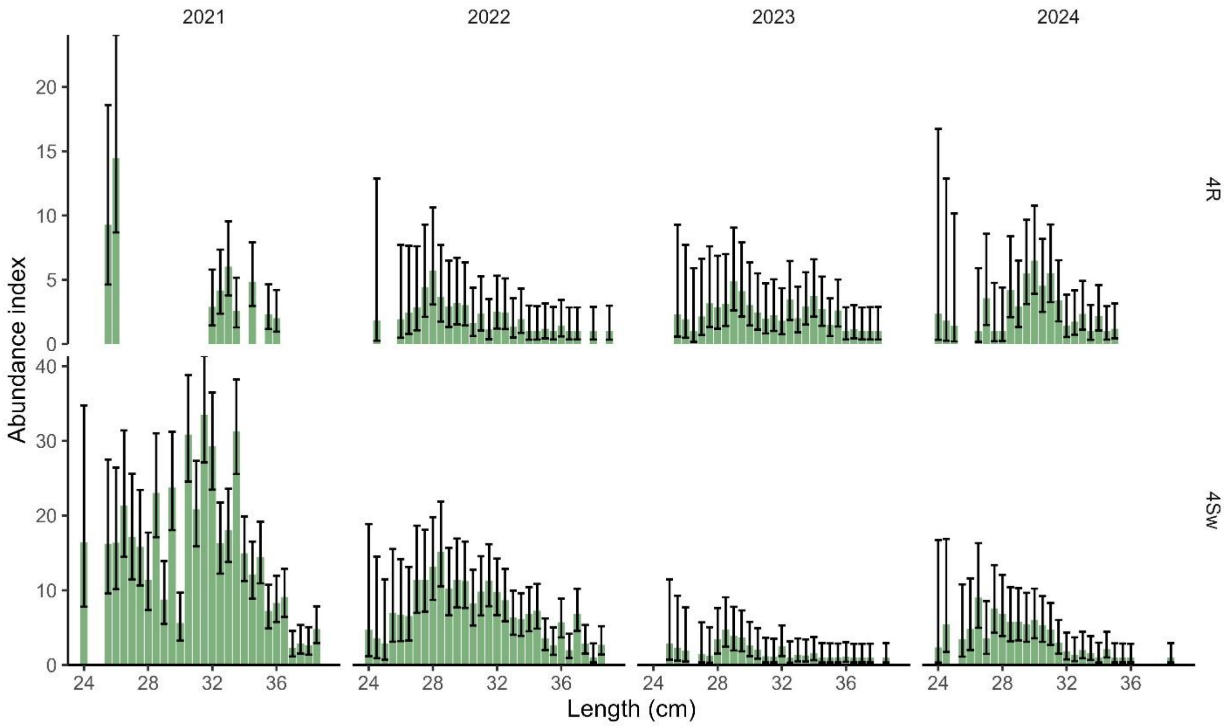

Figure 10 : Model-estimated spring spawner abundance index ($h^{-1} \cdot m^{-2} \cdot 1000$, adjusted for gear selectivity) per length class (cm), year, and region. Vertical bars indicate the 95% confidence interval.

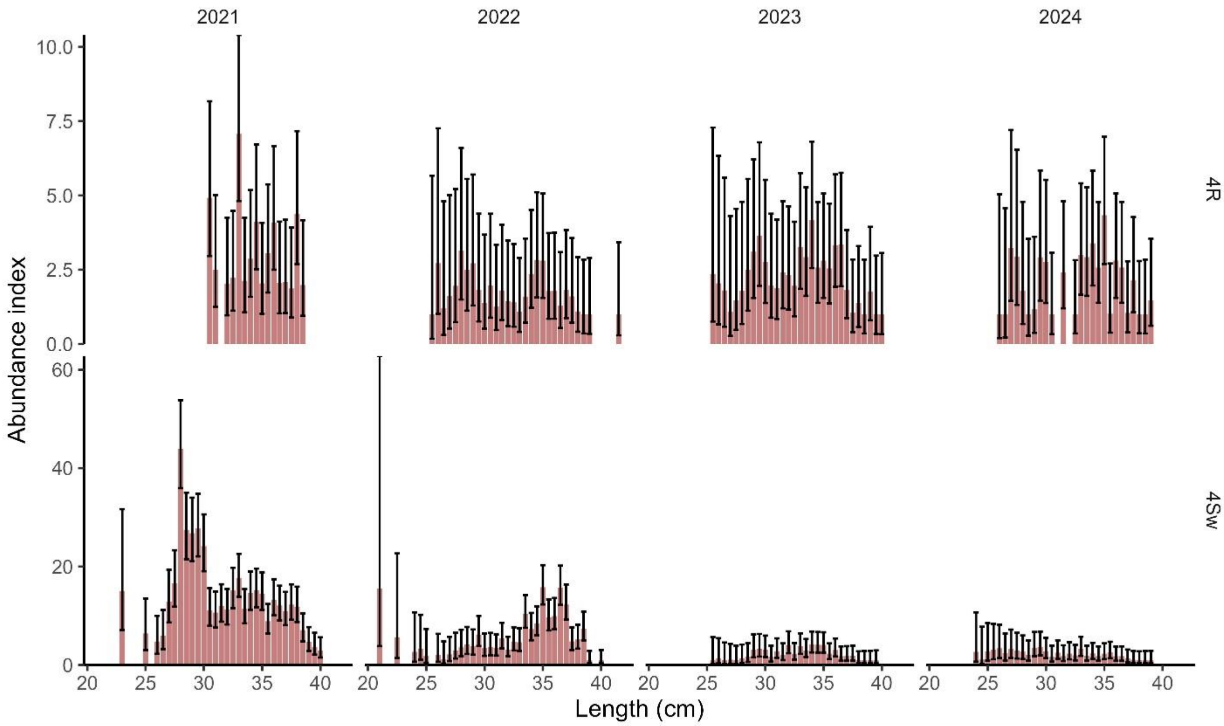

Figure 11 : Model estimated fall spawner abundance index ($h^{-1} \cdot m^{-2} \cdot 1000$, adjusted for gear selectivity) per length class (cm), year, and region. Vertical bars indicate the 95% confidence interval.

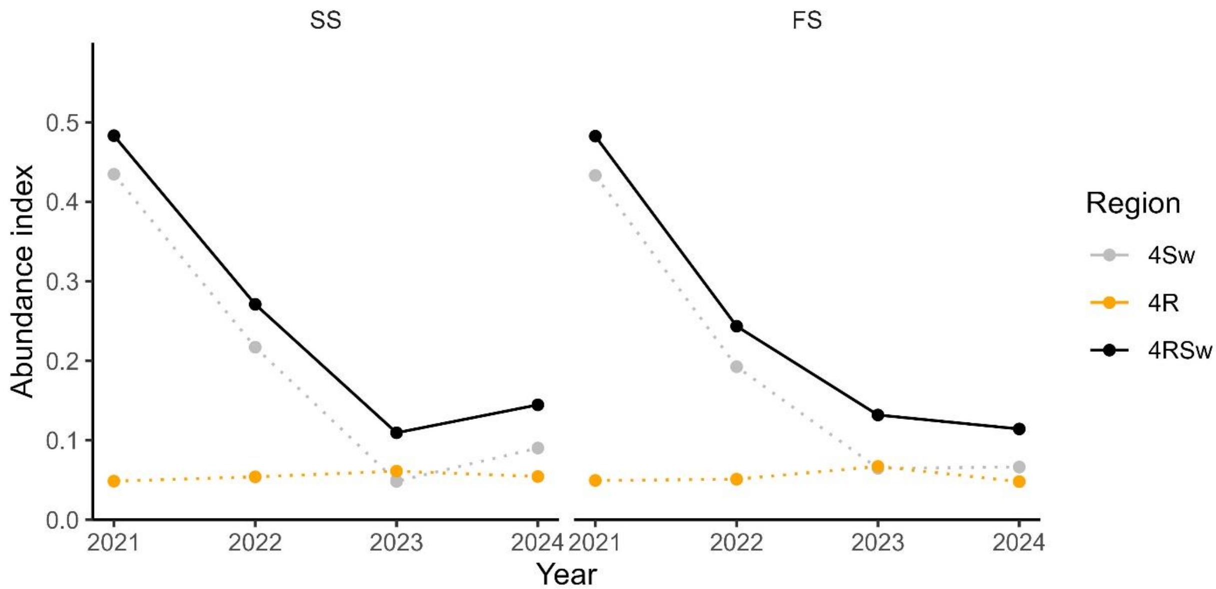

Figure 12 : Relative abundance index ($h^{-1} \cdot m^{-2}$, adjusted for gear selectivity) of spring (SS) and fall (FS) spawning herring, shown separately for each unit area and for both regions combined. No measure of uncertainty is currently available.

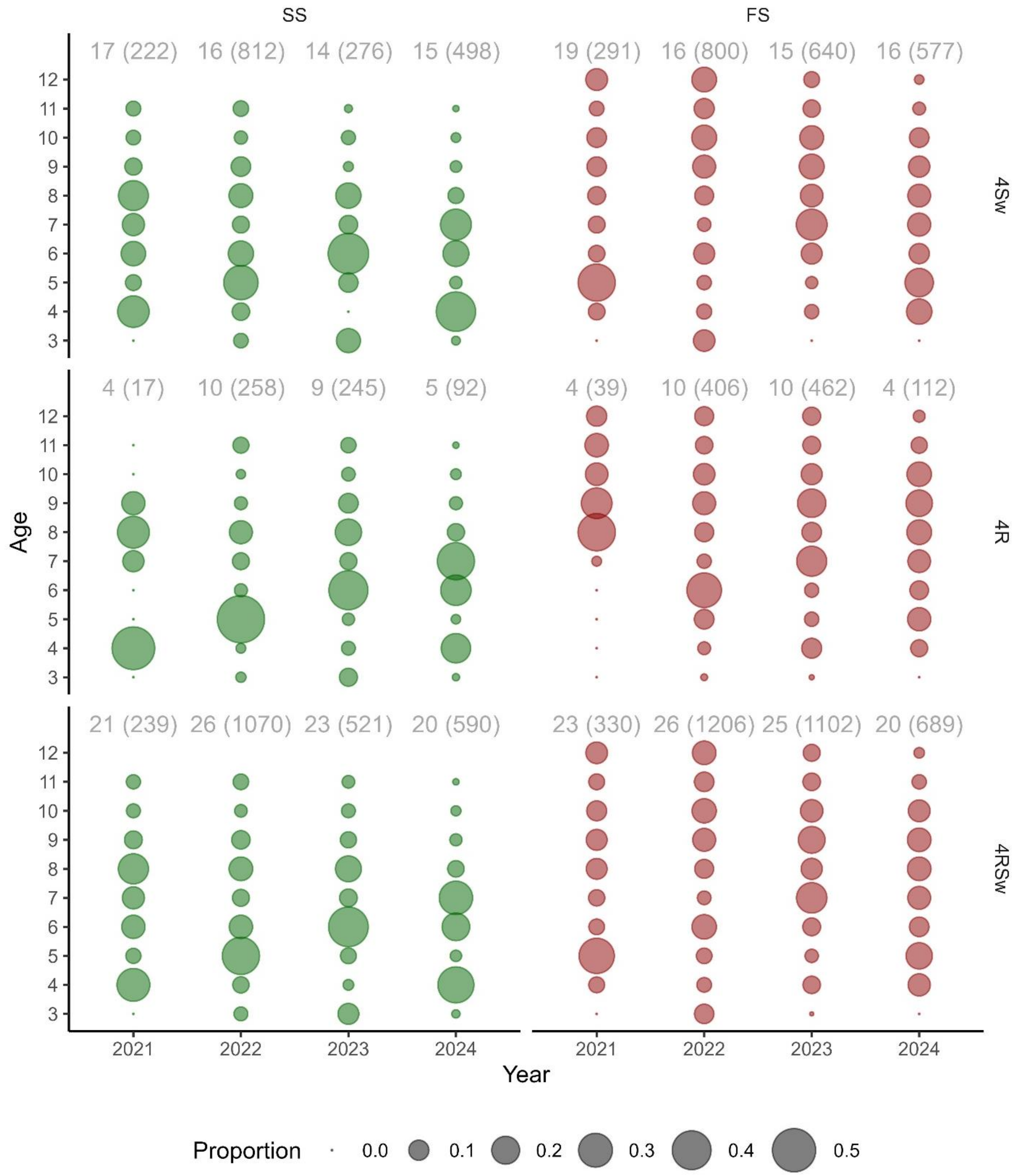

Figure 13 : Abundance-at-age index (annual proportions) of spring (SS) and fall (FS) spawning herring, per region (4Sw and 4R) and overall (4RSw). The annual number of samples and fish caught are indicated in grey. Age 11 and 12 are plus groups for SS and FS, respectively.

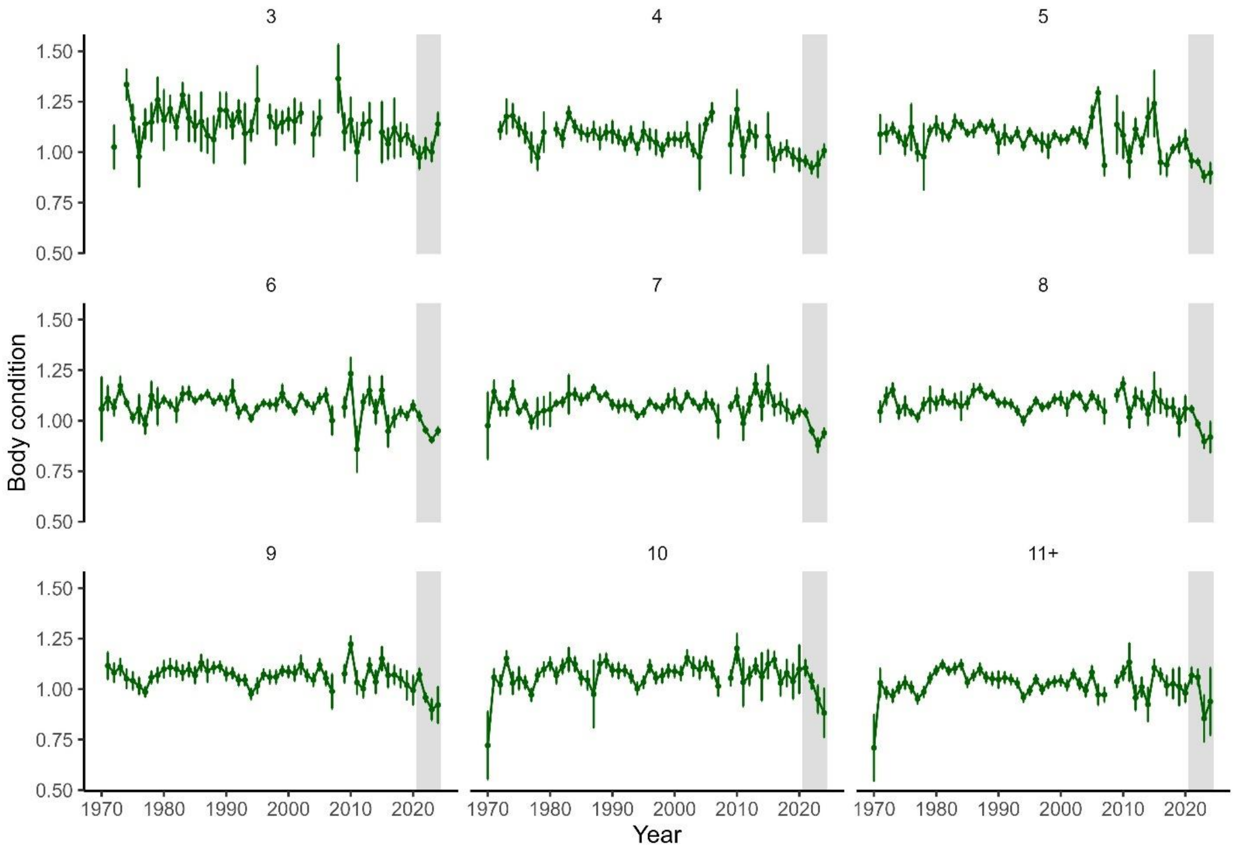

Figure 14 : Time-series of fish body condition (Kn) by age (facets) generated from commercial port sampling data for spring spawners. Vertical bars indicate the 95% confidence interval. Years highlighted in grey correspond to the experimental gillnet survey period.

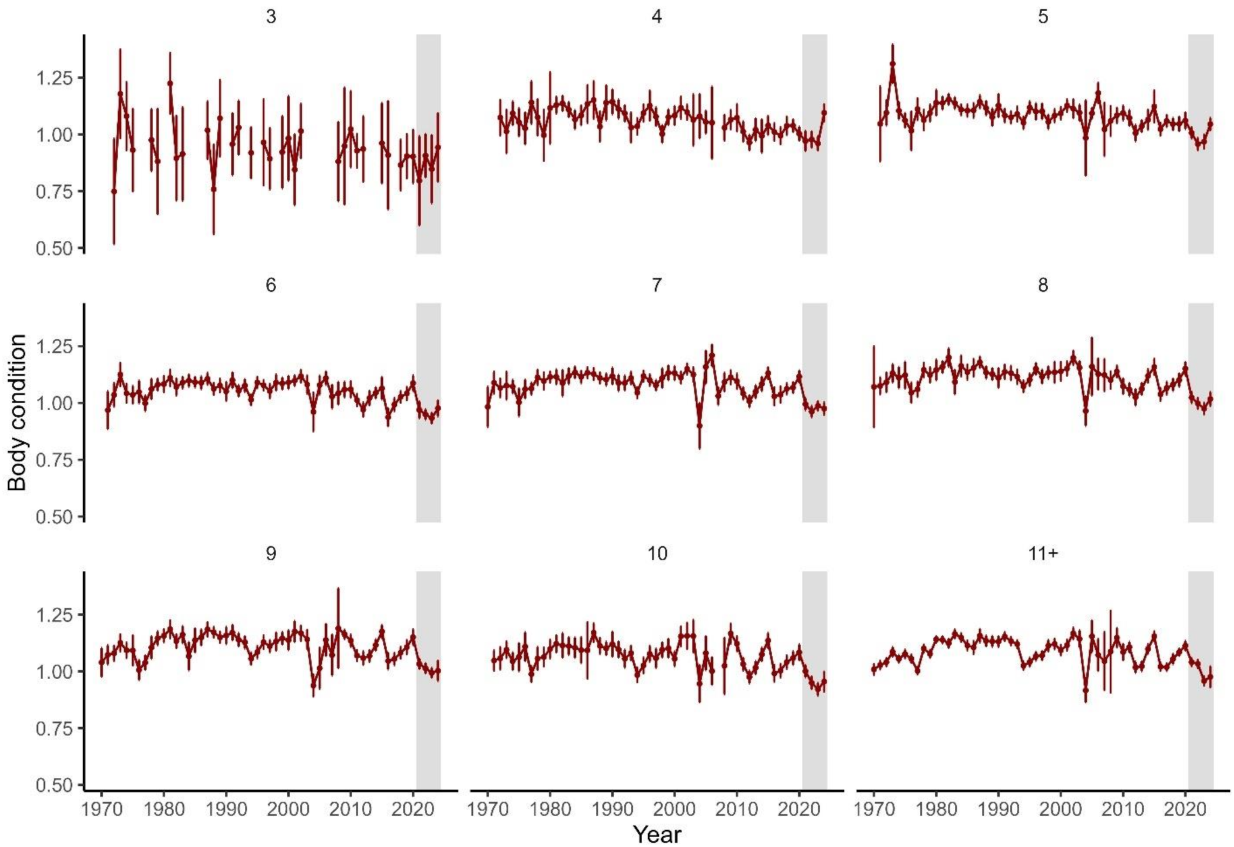

Figure 15 : Time-series of fish body condition (Kn) per age (facets), generated from commercial port sampling data for fall spawners. Vertical bars indicate the 95% confidence interval. Years highlighted in grey correspond to the experimental gillnet survey period.

Figure 16 : Age composition of spring (SS) and fall (FS) spawning herring in two NAFO unit areas (4Ra and 4Rc) observed in commercial (seines), bottom-trawl (multi-species survey), and summer acoustic survey (pelagic trawl) samples collected from June to September. Years prior to 2019 were excluded because of their limited number of samples.

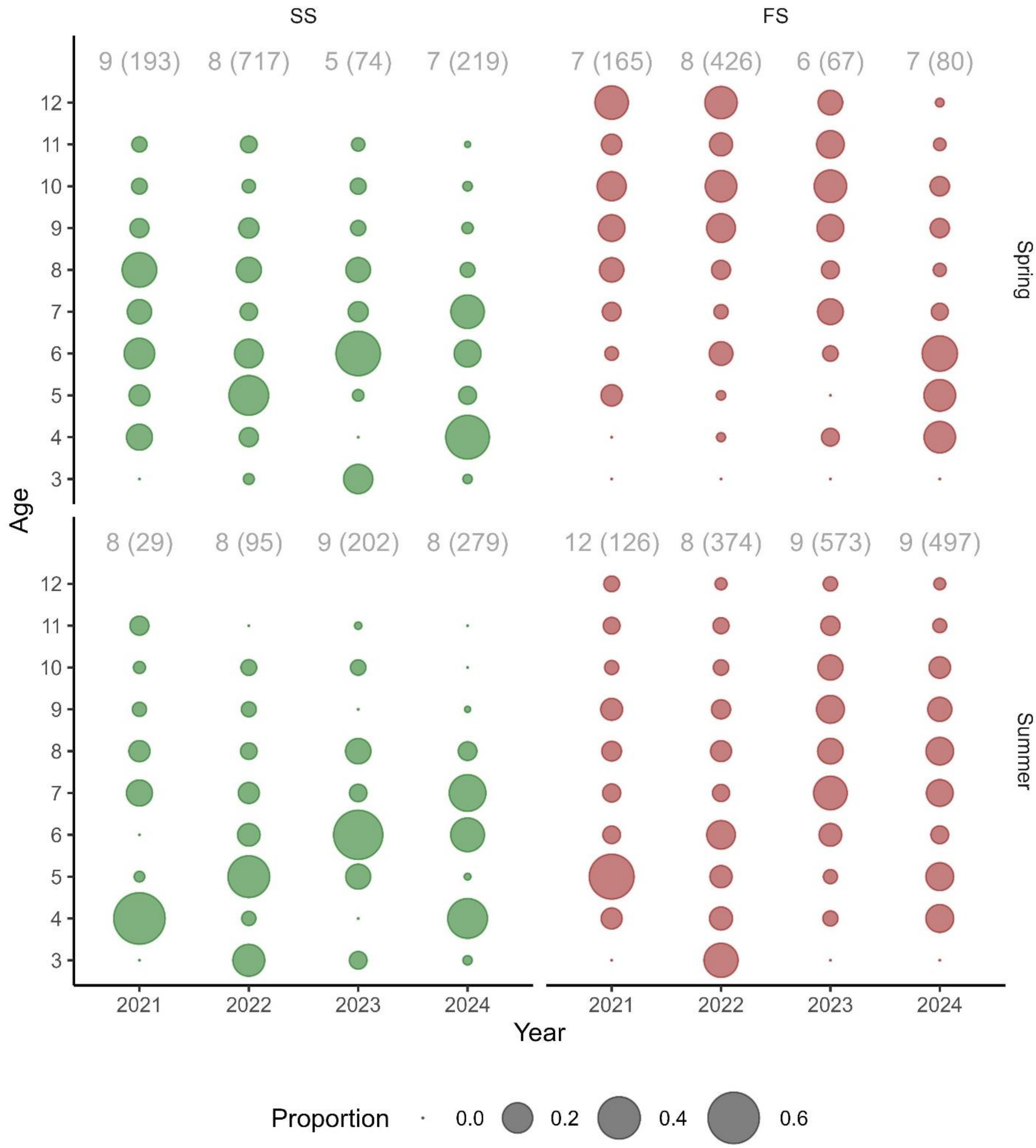

Figure 17 : Abundance-at-age index (annual proportions) of spring (SS) and fall (FS) spawning herring, per period (spring and summer) for NAFO unit area 4Sw. Estimates were generated using the gillnet selectivity model (lowest AIC fit) with a seasonal stratification. The annual number of samples and fish caught are indicated in grey. Age 11 and 12 are plus groups for SS and FS, respectively.

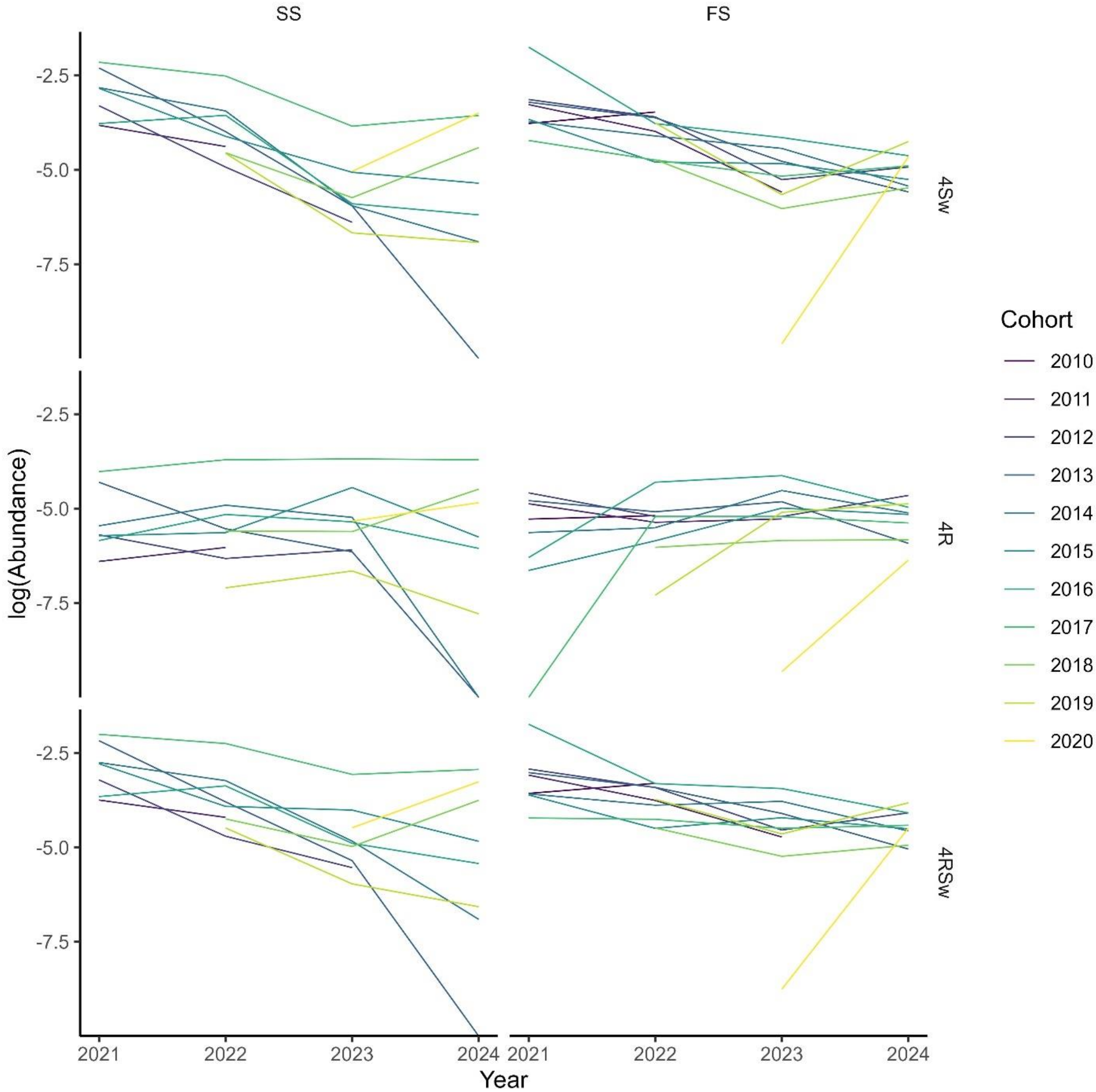

Figure 18 : Regional catch-curve analyses for spring (SS) and fall (FS) spawners.

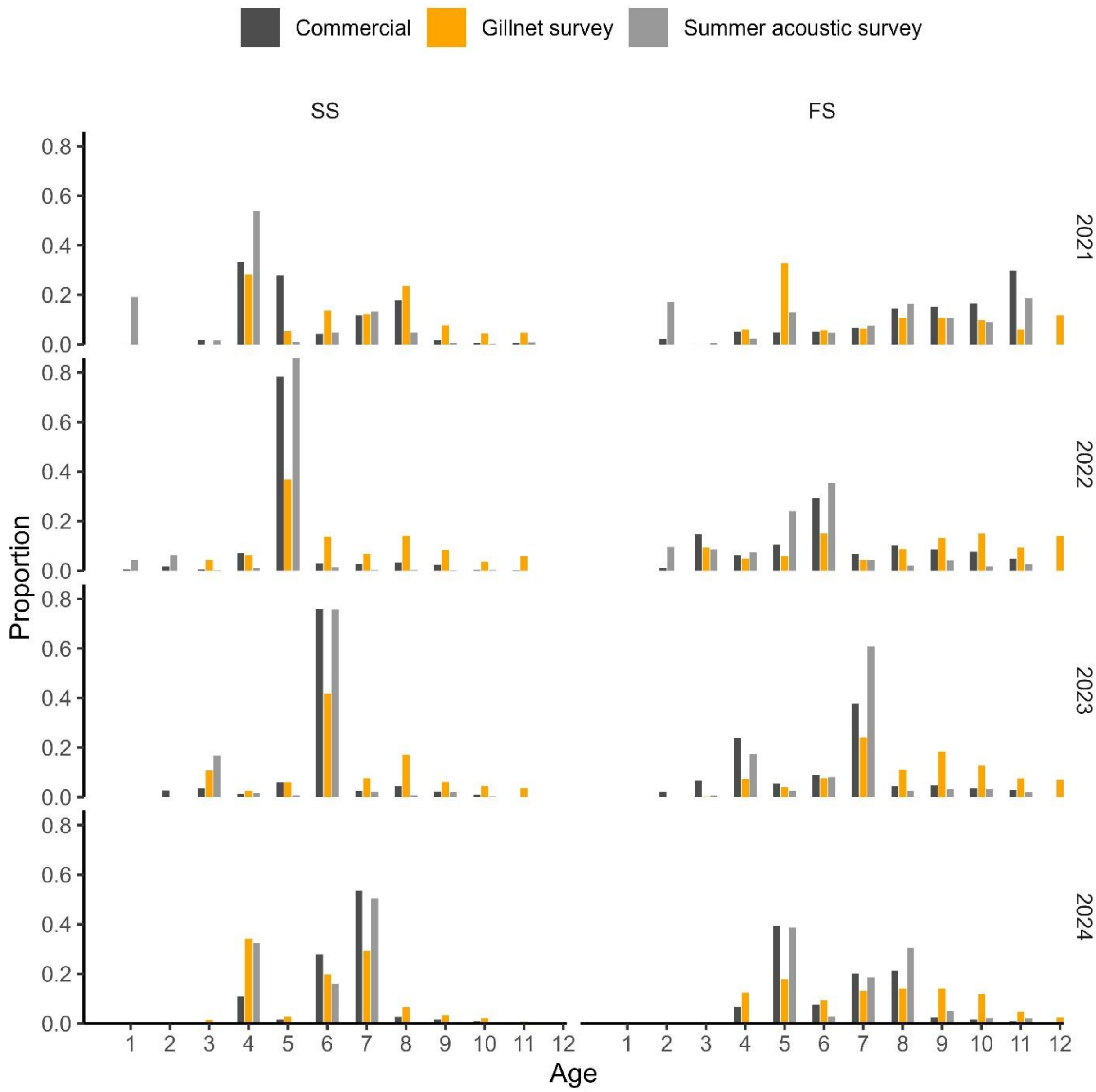

Figure 19 : Annual age composition (proportions) of 4RSw spring (SS) and fall (FS) spawning herring, based on three available indicators: commercial catch-at-age, gillnet survey abundance-at-age, and summer acoustic survey abundance-at-age. The presented data are intended for use as stock assessment model inputs.

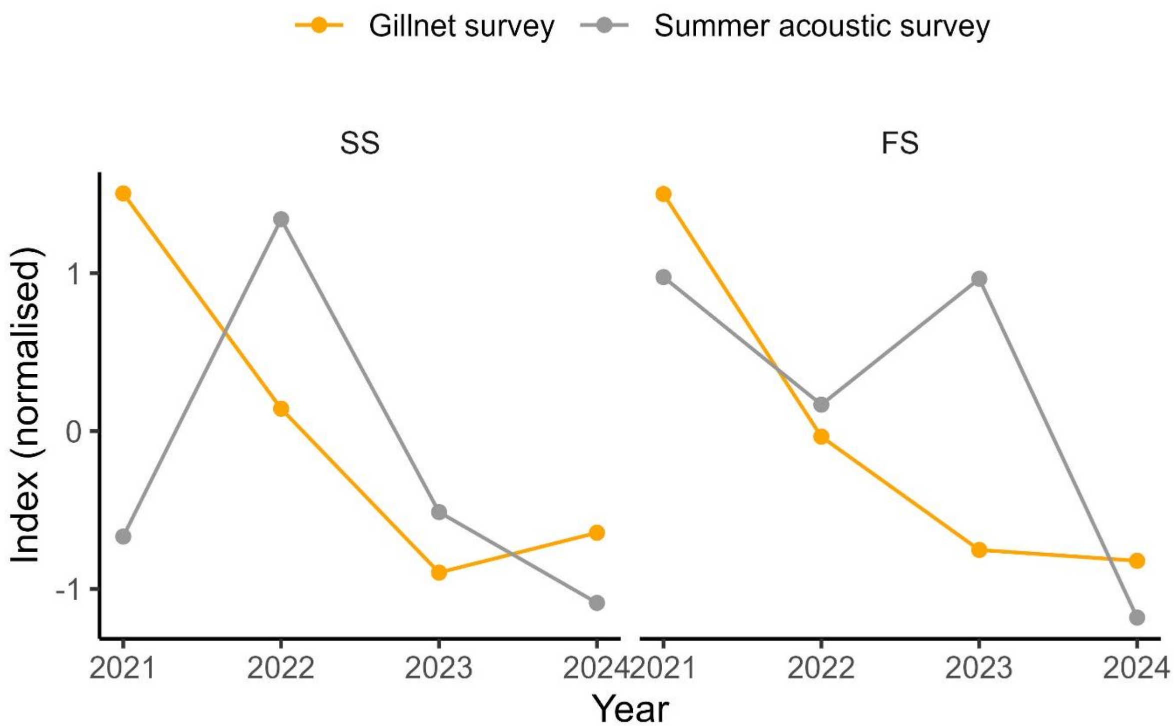

Figure 20 : Normalised abundance indices of 4RSw spring (SS) and fall (FS) spawning herring from the summer acoustic and experimental gillnet surveys.

APPENDIX

Appendix 1 : Selectivity curve equations describing the probability that a fish of a given length (*l*) is retained by a specific mesh size (*m*), ranging from 0 to 1 ($s_m(l)$). Fish length and mesh size were entered in centimetres. Adapted from Millar and Holst, 1997.

Model	Parameters	Equation
Normal fixed	k_1, k_2	$\exp\left(-\frac{(l-k_1 m)^2}{2k_2^2}\right)$
Normal scaled	k_1, k_2	$\exp\left(-\frac{(l-k_1 m)^2}{2k_2 m^2}\right)$
Gamma	k_1, k_2	$\left(\frac{l}{(k_1-1)k_2 m}\right)^{k_1-1} \exp\left(k_1 - 1 - \frac{l}{k_2 m}\right)$
Lognormal	k_1, k_2	$\frac{1}{l}\exp\left(k_1 + \log(\frac{m}{m_1}) - \frac{{k_2}^2}{2} - \frac{\left(\log(l) - k_1 - \log(\frac{m}{m_1})\right)^2}{2{k_2}^2}\right)$